

University of Colorado
Department of Aerospace Engineering Sciences
ASEN 4028
 Project Final Report (PFR)



Vertically Optimized Research, Testing, & EXploration
 May 3rd, 2021
Advisor: Dr. Donna Gerren

Project Customers

Name:	Steve Borenstein
Email:	steve.borenstein@gmail.com
Phone:	303-735-7558

Group Members

Name: Mohamed Aichiouene Email: moai1674@colorado.edu Phone: 720-883-8862	Name: Stephen Albert Email: stal5970@colorado.edu Phone: 303-358-0177
Name: Joe Buescher Email: jobu7780@colorado.edu Phone: 720-331-0852	Name: Bill Chabot Email: william.chabot@colorado.edu Phone: 720-454-4430
Name: Colton Cline Email: cocl0990@colorado.edu Phone: 720-255-8935	Name: Brandon Cummings Email: brcu8751@colorado.edu Phone: 303-882-4382
Name: Roland Ilyes Email: roland.ilyes@colorado.edu Phone: 303-856-8124	Name: Delaney Jones Email: deju1578@colorado.edu Phone: 720-490-7728
Name: Cameron Kratt Email: cakr9969@colorado.edu Phone: 719-351-1003	Name: Michael Patterson Email: mipa0115@colorado.edu Phone: 303-513-0325
Name: Joseph Rooney Email: joro8355@colorado.edu Phone: 309-214-0438	Name: Justin Troche Email: juttr2359@colorado.edu Phone: 718-915-8444

Contents

1	Project Purpose	7
2	Project Objectives and Functional Requirements	7
2.1	Definitions of Success	7
2.2	CONOPS	9
2.3	Functional Block Diagram	10
3	Final Design	12
3.1	Design Requirement Breakdown	12
3.2	Propulsion	19
3.3	Structures	20
3.3.1	Requirements Flow Down	20
3.3.2	Structures System Components	20
3.4	22
3.4.1	Controls	22
3.4.2	Firmware	23
3.5	Autonomous Flight	26
3.5.1	Avionics	28
3.6	Aerodynamics	29
3.6.1	Flight Characteristics Estimation	29
3.6.2	Tail Design	29
4	Manufacturing	32
4.1	Stock Drak Body	32
4.2	Motor Mounts	33
4.3	Empennage	35
4.4	Batteries	36
4.5	Test Stands	37
4.5.1	Static Test Stand	37
4.5.2	Aerodynamic Car Top Test Stand	38
4.6	Other Manufactured Components	40
4.7	Assembly and Integration	41
5	Verification and Validation	42
5.1	Wing Motor Arm Stress Testing	42
5.2	Battery Endurance	45
5.2.1	Static Endurance Test	45
5.2.2	Dynamic Endurance Test	46
5.3	Static Motor Test	47
5.4	Control Test	49
5.5	LiDAR Test	49
5.6	Car Top Aerodynamic Test	50
5.6.1	Setup	50
5.6.2	Procedure	51
5.6.3	Analysis	51

5.7	Hover Testing	52
5.8	Flight Testing	53
6	Risk Assessment and Mitigation	59
7	Project Planning	60
8	Lessons Learned	63
9	Individual Report Contributions	64
	Bibliography	65
9.1	Sensor Conceptual Design	68
9.1.1	Scale Assignment	68
9.2	Firmware Conceptual Design	70
9.2.1	Flight Controller Firmware Criteria Standards	70
9.2.2	FirmWare Scale Assignment	70
9.3	Battery Chemistry Design	72
9.3.1	Battery Chemistry Criteria and Weight Assignment	72
9.3.2	Battery Chemisty Scale Assignmment	73
9.3.3	VTOL Criteria and Weight Assignment	74
9.3.4	VTOL Scale Assignment	74
9.4	Hover Mode Controls	76
9.5	Level Flight Dynamics	76
9.6	Diagrams	77



Preamble

- List of Figures
- List of Tables
- List of Acronyms
- Definition of symbols (nomenclature)

Contents

List of Figures

1	VORTEX Concept of Operations Diagram	9
2	VORTEX Functional Block Diagram	10
3	Propulsion Component Layout Diagram	19
4	Design and Dimensions of the Rear Motor Mount	21
5	Front Motor Assembly with Dimensions	22
6	Controls Verification, PWM Limits Defined on GCS	23
7	ArduPlane Parent Loop Functional Block Diagram	24
8	ArduCopter Autotune Functional Block Diagram	25
9	Mission Planner forward flight loiter test.	27
10	Avionics	28
11	Drag Polar	29
12	FBD For Tail Design	30
13	Tail Design GUI	31
14	Base Drak Components	33
16	Rendering of the full motor arm assembly	35
17	Fully Assembled VORTEX aircraft	35
18	Battery Manufacturing	37
19	Static Test Stand	38
20	Aerodynamic Test Stand	39
21	Aerodynamic Test Stand Interfaces	40
22	Manufactured LiDAR Mounts	40
23	RAPCat System	41
24	Aircraft Wings Along Assembly Process	42
25	Assembled Aircraft	43

26	Motor Arm Stress Testing	44
27	Rear Motor Mount Stress Testing	45
28	Static Endurance Test Results	46
29	Dynamic Testing Thrust Produced and Power Drawn	47
30	Aeronaut vs APC propellers	48
31	Experimental vs Model Comparison for Static Thrust	49
32	LiDAR Test Setup and Results	50
33	Free Body Diagram of Forces on Aircraft During Dynamic Testing	51
34	Flight Testing Timeline	53
35	Google Maps Render of First Flight Test Flight Path	54
36	Hover Thrust Logs from Flight Test 1	54
37	Desired and Actual Roll Plots from Flight Test 1	55
38	Flight Path, Third Flight Test	56
39	RAPCat Launch, Third Flight Test	57
40	Altitude During Autonomous Hover Mission	57
41	RAPCat Launch, Third Flight Test	58
42	Primary Risks of VORTEX Project	59
43	Org Chart	60
44	WBS	61
45	Gantt Chart	62
47	Hover Mode Response to Other Perturbations	76
48	Linearized Lateral Matrix	76
49	ArduCopter Parent Diagram	77
50	L1 Navigation Controller Functional Block Diagram	78
51	Total Energy Control System (TECS) Functional Block Diagram	79

List of Tables

1	Objectives Table for Levels of Success	8
2	Overview of Manufacturing	32
3	Base Drak Wing Kit Components	33
4	Tail Manufacturing Overview	36
5	Brand and Size of Propellers Tested	48
6	Report Contributions	64
7	Landing Sensor Trade Study Weighting	68

8	Scale Assessment of Landing Sensors	69
9	Firmware Trade Study Weighting	70
10	Scale Assessment of Flight Controller Firmware Criteria	71
11	Trade Study Battery chemistry Weighting	72
12	Scale Assessment of Battery Composition	73
13	Rotor Configuration Weighting	74
14	Scale Assignment for VTOL Configuration	75

List of Acronyms

AoA	-	Angle of Attack
CAD	-	Computer-Aided Design
CFD	-	Computational Fluid Dynamics
COTS	-	Commercial off-the-shelf products
EKF	-	Extended Kalman Filter
ESC	-	Electronic Speed Controller
FBD	-	Functional Block Diagram
FEA	-	Finite Element Analysis
FEM	-	Finite Element Modeling
GPS	-	Global Positioning System
IRISS	-	Integrated Remote and In-Situ Sensing
PAB	-	Project Advisory Board
PCB	-	Printed Circuit Board
PETG	-	Polyethylene terephthalate glycol
RAPCat	-	Rapid Aircraft Pneumatic Catapult
TECS	-	Total Energy Control System
TWR	-	Thrust to Weight Ratio
UAS	-	Unmanned Aerial System
VORTEX	-	Vertically Optimized Research, Testing, and EXploration
VTOL	-	Vertical Take Off and Landing
WBS	-	Work Breakdown Structure

Nomenclature

C	-	Capacity
S	-	Cells in series
P	-	Cells in parallel
R_i	-	Cell impedance
V_0	-	Cells initial voltage
K1	-	Slope of linear fit curve of voltages vs discharge capacity
n	-	peukert's coefficient

1 Project Purpose

Section Authors: Bill Chabot, Cameron Kratt

The Integrated Remote and In-Situ Sensing (IRISS) group based at the University of Colorado Boulder is responsible for the collection of meteorological data through the use of a fleet of unmanned aerial vehicles. The data gathered from these missions are used to improve supercell thunderstorm models and tornado detection capabilities. Examples of their existing aircraft and mission information can be found on their website[2]. The current UAS launch protocol involves a car-mounted pneumatic launch or a bungee-powered system. While these methods provide benefits to ease of takeoff, they certainly come with drawbacks as well. The launch site must be accessible by road and significant clearance is required around the launch vehicle. Current versions of their UAS's perform a skid-stop landing, which inhibits the ability to deploy a payload or land in smaller areas. The VORTEX (Vertically Optimized Research, Testing, and Exploration) vertical takeoff and landing (VTOL) platform is designed to satisfy these restrictions and broaden the capabilities of IRISS. A vertical takeoff does not require a pneumatic or bungee launch and requires minimal clearance surrounding the launch site, adding significant versatility. Hover flight capability allows for the deployment of a payload as well as safer emergency flight termination. By designing modifications to an existing airframe, IRISS will be able to expand their operational capabilities without placing significant burden on the team to design and manufacture additional units. A key aspect to this project is utilizing rapid, repeatable 3D printing for the bulk of the modifications. This will allow IRISS to quickly and cheaply manufacture several future units for simultaneous operation.

2 Project Objectives and Functional Requirements

Section Authors: Bill Chabot, Michael Patterson, Justin Troche, Cameron Kratt, Joseph Buescher

2.1 Definitions of Success

A key part of the progression of the Senior Design course and development of any system is the understanding of what success means. For the purpose of this project, the customer's requirements were broken into seven categories: Flight, Budget, Endurance, Airframe, Avionics Electronics, Autonomy, and Safety. Success for the flight category will be indicated by the propulsion system demonstrating sufficient thrust in hover, capability to transition from vertical to horizontal flight, and RAPCat compatibility. The customer has specified a desire for a per unit cost not to exceed \$1000 but has indicated that if it is deemed necessary and justified, some additional margin on the budget may be possible. For endurance, the propulsion system must demonstrate its ability to perform for the expected duration of the demonstration mission. The airframe must withstand the expected forces of RAPCat launch, mission execution, as well as a specific customer request of 10G loading in the vertical direction. The avionics package must demonstrate its ability to control all flight surfaces and motors, as well as interpret the data from the sensors to use for primary flight control. The mission must be performed autonomously, so the aircraft must demonstrate its ability for the flight computer to execute a preprogrammed mission while maintaining communications with the ground stations, and having a safety mode flight profile referred to as autonomous return to loiter (RTL). A functioning prototype, capable of achieving the functional requirements detailed

below, is to be delivered to IRISS at the end of the project.

Table 1: Objectives Table for Levels of Success

	Level 1	Level 2	Level 3
Flight	Show on a static test stand that the propulsion system is capable of producing enough thrust to provide a TWR greater than 1	Maintain tethered hover at 2 m of altitude for 30 seconds as well as demonstrate capability to transition to horizontal flight while aircraft is mounted to a test stand	Aircraft shall demonstrate takeoff ability via RAP-Cat launch system as well as demonstrate full transition from vertical to horizontal flight modes.
Budget	The aircraft shall cost no more than \$1250, not including IRISS avionics package.	The aircraft shall cost no more than \$1000, not including IRISS avionics package.	The aircraft shall cost no more than \$900, not including IRISS avionics package.
Endurance	The propulsion system shall maintain required thrust output for the equivalent of 1 hour cruise and 2 takeoffs and landings (approximately 1 hr 16 minutes) on a static test stand in simulated freestream conditions of 18 m/s with >15% battery remaining	-	Demonstrate 1 hour of flight cruise as well as 2 takeoffs and landings
Airframe	A finite element analysis of the modified airframe will be performed to demonstrate that it can withstand the required forces with a FOS of 1.7	The aircraft will have full integration capabilities with RAPCat launch system, and show that it can withstand the forces due to acceleration.	The airframe shall withstand axial and lateral forces up to 10G.
Avionics & Electronics	All motors and actuators shall be successfully integrated with the flight controller. The telemetry link shall be maintained with less than 25% packet loss within 1 km of the ground station.	All external (non-native) sensors are successfully integrated with the avionics system.	-

Autonomy	Both the VTOL and fixed-wing modes have valid dynamic models to ensure active stabilization is possible. Ensure that the chosen avionics package interfaces successfully with propulsion system, sensors, and connectivity with ground station.	The aircraft can autonomously execute a takeoff and landing.	The aircraft shall autonomously execute a full mission profile, transitioning between flight modes, and land within a 1.5 meter radius of a target location.
Safety	The aircraft shall have an autonomous return to loiter function if telemetry is lost for an extended period (90 seconds) as well as capability to terminate the flight immediately upon command from the GSE		-

2.2 CONOPS

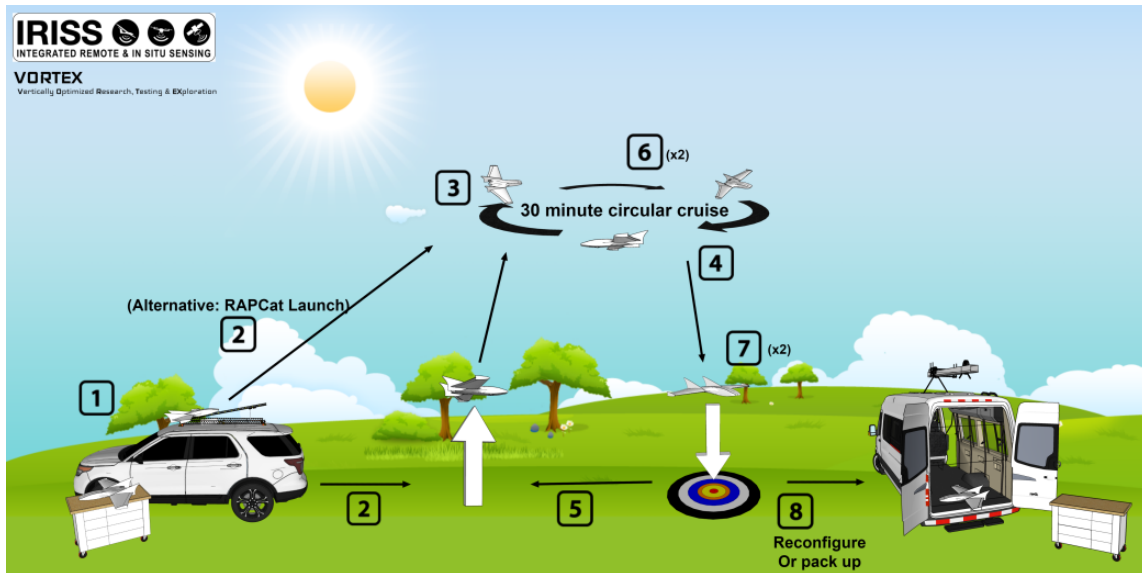


Figure 1: VORTEX Concept of Operations Diagram

The figure above is the VORTEX concept of operations diagram. The primary focus of this project is the successful implementation of a VTOL system on the Drak wing set. As this vehicle

will share the same Drak base of the RAAVEN platform, it will maintain its current capabilities with the RAPCat launch system with no additional transportation or launch infrastructure required to accommodate the VTOL version. Once the system is transported to its operational location, it will be configured for flight by connecting the on-board computer to a ground station (e.g. a laptop computer) and uploading the desired mission profile. After the computer is configured, the vehicle is set up for deployment before executing either a vertical takeoff or RAPCat launch. Once airborne, the vehicle will transition to horizontal flight mode and perform a circular cruise for 30 minutes. After 30 minutes, the vehicle will then transition and perform a vertical landing at a specified target location, within 1.5 meters of the target. After a brief moment, the vehicle will perform the second (or first depending on initial launch) vertical takeoff, transition to horizontal flight and perform the second 30 minute circular cruise. Upon completion of the second cruise, the vehicle will return to the specified end of mission location, transition, perform the second vertical landing and then be packed up for transport. A successful mission is comprised of 2 vertical takeoffs, 2 vertical landings and 1 hour total endurance split into 2 30 minute cruises.

2.3 Functional Block Diagram

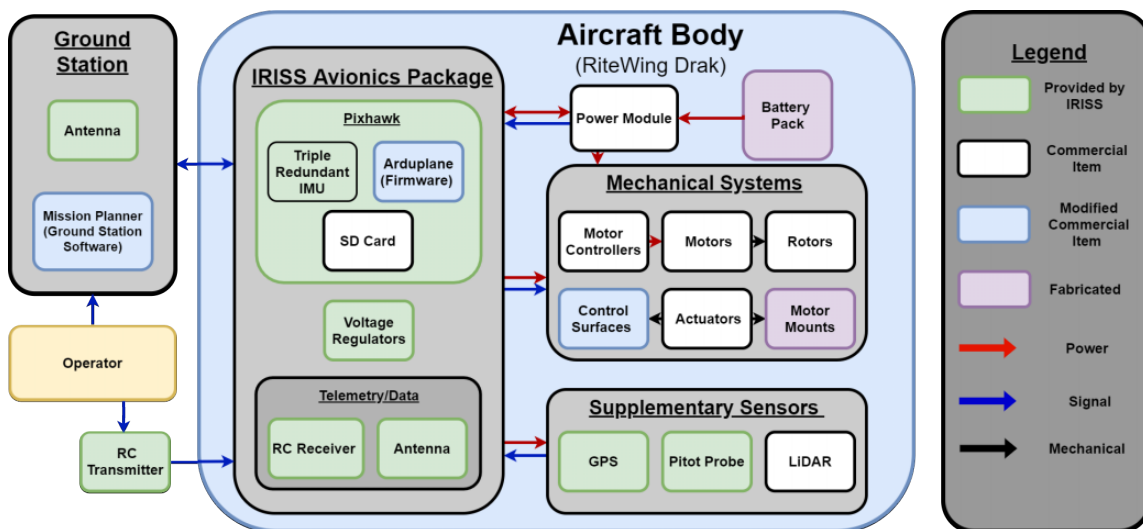


Figure 2: VORTEX Functional Block Diagram

Our custom lithium-ion battery pack, which will be discussed more in depth in Section 7, powers the avionics system via a power module provided by IRISS. All aspects of the avionics system was provided by IRISS, except the LiDAR and forward tilt motors and servos, and electronic speed controllers. The battery pack also provides power directly to the three electronic speed controllers, which govern propeller speed. The voltage regulators included in the avionics system step the voltage down in order for the flight controller and peripherals to function. In manual pilot mode, the RC receiver receives commands from the RC transmitter and passes them along to the flight controller. The flight controller processes these commands and relays them to the electronic speed

controllers and servo motors, which govern control surfaces via pulse width modulation output ports. In autopilot mode, the flight controller uses information from the GPS, pitot probe, and IMU's to automatically send commands to the electronic speed controllers and servo motors in order to execute the mission profile uploaded from the ground system prior to flight. The provided custom telemetry package relays aircraft state information as well as atmospheric sensor measurements back to the ground station during flight. A LiDAR rangefinder provides altitude data to facilitate accurate and gentle vertical takeoffs and landings. The green items indicate hardware provided by IRISS, and white items are commercially procured. Components highlighted in blue and purple are items that will be modified or manufactured by the VORTEX team to meet customer goals. Components critical to project success include the custom battery pack, front tilting motors and LiDAR.

The following list lays out the functional requirements developed for this project as well as rationale for their inclusion. The design requirements flow-down can be seen in Section 6 of the report.

- **FR 1: The aircraft shall be a VTOL conversion of the COTS RiteWing RC “Drak” airplane kit.**
Rationale: Both the critical pieces of this requirement, the "VTOL conversion" and "Drak airplane kit" are requirements supplied by the customer, IRISS. VTOL conversion is the primary novel part of the project, so it is a key element.

- **FR 2: The aircraft shall have an endurance of one hour in addition to two takeoffs and landings.**
Rationale: IRISS has expressed the desire for the VTOL aircraft to be able to perform an intermediate vertical landing and takeoff during the mission. In order to gain sufficient atmospheric measurements, the aircraft must have an endurance of one hour.

- **FR 3: The aircraft shall be able to autonomously execute all aspects of its mission from takeoff through landing.**
Rationale: The goal is to have an autopilot controlled aircraft that can execute missions for IRISS and any clients of IRISS. The system is supposed to be easily used in any situation or application so automation is key for a successful mission.

- **FR 4: The aircraft shall maintain communication with the ground station up to a distance of 2km. (In this context, maintaining communication is indicated by <50% packet loss).**
Rationale: It is necessary to the customer that the means of communication on the aircraft are capable of reporting enough valid data back to the ground station computer during the flight, this includes the telemetry transmitter and command receiver. The distance is what the provided telemetry package is capable of and the project must not let any design solutions interfere with its functionality.

- **FR 5: The aircraft shall be capable of carrying a 0.5 kg payload.**
Rationale: It is a customer request to support the addition of 0.5 kg which represents an

available space in the mass budget for more scientific instruments/sensors.

- **FR 6: Aircraft shall be capable of taking off from existing RAPCat launch system.**

Rationale: It is a customer requirement that the VTOL aircraft still be capable of taking off from the existing RAPCat launch system. The RAPCat launch is a more efficient use of battery power than a vertical takeoff and will be used when available.

- **FR 7: The airframe, propulsion system, and required mounting hardware shall cost no more than \$1000 per aircraft.**

Rationale: The customer's goal is to be able to manufacture individual units of the VTOL converted Drak at an economically feasible price of no more than \$1000. This budget does not include the provided avionics package as it is currently in use in other aircraft in IRISS fleet and is already manufactured by them. This also does not include batteries as they already have purchased battery packs on hand and also have the capability to fabricate their own battery packs. The RiteWing Drak kit must be included in the unit cost as each time the VTOL aircraft is to be fabricated, a Drak kit must be purchased for modification.

3 Final Design

Section Authors: Roland Ilyes, Cameron Kratt, Joseph Rooney, Mohamed Aichiouene, Delaney Jones, Joseph Buescher, Brandon Cummings, Bill Chabot

3.1 Design Requirement Breakdown

FR1: The aircraft shall be a VTOL conversion of the COTS RiteWing RC "Drak" airplane kit

Motivation: Both the critical pieces of this requirement, the "VTOL conversion" and "Drak airplane kit" are requirements supplied by the customer, IRISS. VTOL conversion is the primary novel part of the project, so it is a key element.

Verification: Verifying the VTOL conversion will require ensuring the propulsion and stability systems are capable of maintaining stable flight in both the vertical and horizontal flight modes, as well as transitioning between them. Verifying that the final product is modified from the Drak kit can be done by inspection and making sure that the original Drak fuselage is present in the final design.

- **DR 1.1: The aircraft shall be able to sustain hover using its own thrust system**

Motivation: For the VTOL requirement, the ability to vertically takeoff and land requires a stable hover configuration after taking off or before landing.

Verification: This will be verified using a full system test using a tethered hover flight.

- **DR 1.2: The aircraft configuration is capable of VTOL to horizontal flight transition**

Motivation: While VTOL is an important part of project as a whole, the largest part of the flight profile is a horizontal flight mode. Being able to transition between horizontal and vertical flight modes is critical for the entire mission.

Verification: The flight controller will rotate thrust vector from horizontal to vertical and vice versa on a static test stand and/or during flight.

- **DR 1.3: All components shall mount to a modified Drak airplane kit**

Motivation: Measuring whether the final project is a modification of the Drak kit is easiest performed by making sure that all components that are manufactured by the team can fit to the modified stock Drak kit.

Verification: Insure that all components on the final aircraft are connected, directly or indirectly, to a piece of the stock Drak kit, modified or otherwise.

- **DR 1.4: Modified kit shall require fewer than 20 person-hours to assemble a full unit**

Motivation: IRISS wants assembling this kit to be done by undergraduates in their labs after it is done. In order to facilitate this, the manufacturing and assembly processes should be simple enough that 20 person-hours or less for people with some experience in building RC aircraft.

Verification: Have a team of people assemble the full unit while keeping time. The total man hours should be less than 20 (i.e. if there are 10 people working on assembly, then it should be completed in less than 2 hours).

FR 2: The aircraft shall have an endurance of one hour in addition to two takeoffs and landings.

Motivation: IRISS has expressed the desire for the VTOL aircraft to be able to perform an intermediate vertical landing and takeoff during the mission. In order to gain sufficient atmospheric measurements, the aircraft must have an endurance of one hour.

Verification: Successful performance of the test mission outlined in the CONOPS.

- **DR 2.1: The aircraft shall possess an internal power system capable of powering all electronics necessary for a single flight.**

Motivation: The power system must be able to power all necessary electronics without swapping out or recharging mid mission.

Verification: Each hardware component of the power system is enclosed inside the aircraft. Actuators and motors are tested to be receiving power.

- **DR 2.2: The propulsion system shall support sustained horizontal flight for a minimum of one hour at standard operating loads.**

Motivation: IRISS desires one hour of flight time in order to acquire sufficient atmospheric

measurements.

Verification: During flight or a static test imitating flight conditions, the propulsion system will function for an hour.

- **DR 2.3: The propulsion system shall be capable of two vertical takeoffs and landings.**

Motivation: IRISS wants the ability to perform a mid-mission landing and takeoff, which totals two takeoffs and landings.

Verification: During a static test the propulsion can generate the required thrust for 2 takeoffs and 2 landings on a single battery.

- **DR 2.4: The propulsion system shall generate sufficient and sustained thrust to overcome the expected drag forces on the aircraft in vertical and horizontal flight.**

Motivation: In order to reach a safe altitude and speed for flight, the propulsion system must provide sufficient thrust.

Verification: During a static test, the propulsion system will generate thrust exceeding the predicted force models in separate vertical and horizontal configuration.

- **DR 2.5: Power system shall have >10% capacity remaining on completion of mission.**

Motivation: In order to prevent potential damage, the power system must not fully deplete after a mission. This allows room for contingency and unknown risk

Verification: After the mission or full duration static test, the remaining power will be measured to be greater than 10% of full battery capacity.

- **DR 2.6: Aircraft can complete entire mission on one set of batteries without charging or replacing.**

Motivation: Needing to replace the battery mid-flight defeats the purpose of the ability to vertically land and takeoff at another location. Mission continuity and data collection is a priority.

Verification: The aircraft is able to complete a full mission or static test equivalent without power alteration or replacement.

- **DR 2.7: Aircraft cruise speed shall be at least $16 \frac{m}{s}$.**

Motivation: To prevent stall, the aircraft must cruise at a speed of at least $16 \frac{m}{s}$.

Verification: The flight speed during cruise will be reported to be greater than or equal to $16 \frac{m}{s}$ from the ground station equipment.

FR 3: The aircraft shall be able to autonomously execute all aspects of the mission profile from takeoff to landing.

Motivation: The goal is to have an autopilot controlled aircraft that can execute missions for IRISS and any clients IRISS has. The system is supposed to be easily used in any situation or application so automation is key.

Verification: First by preparing the flight software to control the specific aircraft, the second is affirming the creation of a mission profile that is required for the success of this aircraft, and finally performing the mission profile while on a fixed test stand prior to a flight test.

- **DR 3.1: The aircraft shall autonomously takeoff once the operator/pilot starts the flight**
Motivation:
Verification: Construct a working mission profile simulation and ensure that the motors and other mechanisms are behaving properly while the craft sits on a test stand. Further flight testing will be necessary for full verification.
- **DR 3.2: The on-board flight controller shall the control propulsion system and flight surfaces**
Motivation: For the system to be fully autonomous and properly execute missions, the flight controller must be able to apply proper thrust, deflect control surfaces, and handle sensor data.
Verification: This can be done by checking that the servos and motors are behaving properly once given a mission profile with the aircraft stationary on a test stand. A full flight test will also be required to ensure that the gains are properly tuned and the system behaves nominally.
- **DR 3.3: The aircraft shall autonomously transition between vertical and level flight modes**
Motivation: This design requirement is a crucial facets of the automation functional requirement sets up the creation of the firmware parameters, choosing the correct control mechanisms, and facilitates the creation of simulations/models to predict the response. There is a lot of risk during transition especially, so this design requirement is very important as it keeps all these aspects in the mind of the designers.
Verification: To demonstrate that this design requirement can be met requires analysis and physical testing. Analysis entails effectively modeling the dynamics of transition via simulation and dynamics models to estimate what the nominal response should be and to show potential risks. Demonstration can be done in two ways: obviously through a full flight test, but also by ensuring that the mechanisms act properly alone after given a mission profile to execute. This can be done on a test stand.
- **DR 3.4: The aircraft must be capable of having of less than 10cm accuracy of relative altitude when the aircraft is below 5m GPS relative altitude**
Motivation: This design requirement facilitates the need for accurate range finding sensors to ensure that takeoffs and landing are done without crashing or failure. If the relative altitude of GPS is only used, this can become an issue as GPS is known to have a typical error of greater than 1m, and this can become an issue during landing and takeoff. Above 5m, the GPS can take over but more accurate sensor data is required when the aircraft is closer to the ground.
Verification: This requirement can be verified this by the data sheet specifications of the chosen sensor, physically verifying the sensors specified accuracy above various surfaces, and analyzing flight logs from both IRISS flights and the team's own flights.
- **DR 3.5: The aircraft shall be capable of completing a prescribed mission profile without pilot input after initial flight configuration**
Motivation: This requires that the aircraft must be able to handle any mission profile prescribed to it. This requires that the system is accessible to any client and adaptable. This is will make the final product more easily marketable and widely used.

Verification: Changing the mission profile and showing that the system is capable of completing the different runs is the main method of verification. Checking data logs and ensuring that the system is behaving nominally is another form of verification for this design requirement.

- **DR 3.6: The aircraft shall be able to recognize ground station location and distances with 2m accuracy relative to GSE**

Motivation: Design requirement 3.6 is a specification that the GPS shall provide positional accuracy of 2m throughout the mission. This is desired as the flight software utilizes position for its calculations throughout flight, and in order to meet DR 3.4, it is required that the relative altitude is known from the GPS prior to reaching 5m above the ground. The GPS must be capable of providing confidence that the sensor that satisfies DR 3.4 will be given priority reporting of the relative altitude data that is used by the flight software for landing calculations. This is necessary so the more accurate reading, the sensor for DR 3.4, is reporting data in order for the aircraft to have a gentle controlled landing.

Verification: This will be verified with the testing of the telemetry package at a known short distances of 50km and 100km.

- **DR 3.7: The aircraft shall autonomously land at target location**

Motivation: The final design requirement states that the aircraft must be capable of landing at a target location. The importance of this requirement is so that the aircraft can land in a chosen location that will make it easily retrievable, and allow for it to be landing in a spot that will not damage the aircraft in any way (such as a dirt clearing without objects).

Verification: The verification of this is demonstrating in the mission setup that a location can be chosen from a map of satellite images, and once the aircraft is in a capable state, proving a takeoff, hover, translate, and landing at chosen locations in the mission planner software.

Functional requirement 3 is the driving force behind all automation for this project. It encompasses requirements that range from physical behavior of the system, sensor data, mission execution, and accessibility to clients. From functional requirement 3, the most important design requirements flow down. DR 3.1 gives requirements for the VTOL capabilities, 3.2 deals with active control mechanisms and requires them to be robust, 3.4 and 3.6 deal with the sensors and telemetry for the system, and 3.3/3.5 deal with mission execution and configuration. With these requirements filled out, the design process can begin with the functional and design goals in mind.

FR 4: The aircraft shall maintain communication with the ground station up to a distance of 2km. (In this context, maintaining communication is indicated by <50% packet loss).

Motivation: It is necessary to the customer that the means of communication on the aircraft are capable of reporting enough valid data back to the ground station computer during the flight, this includes the telemetry transmitter and command receiver. The distance is what the provided telemetry package is capable of and the project must not let any design solutions interfere with its functionality.

Verification: The aircraft shall be taken 2km away after being activated so that it is reporting data, and the packet loss must be less than 50% once the aircraft is away. This will be discussed more further on.

- **DR 4.1: GS shall be capable of receiving commands and recording telemetry from onboard sensors**

Motivation: The aircraft must be controllable from Pilot input, and during the flight it is required that all of the data that ArduPilot records from the flight controller is reported so that the operator can notice if anything is out of the ordinary.

Verification: Specific commands will be sent through the controller used for the test flights to prove that the receiver is functioning, and the transmitter will be proven to work if it reports the data log for the tests.

- **DR 4.2: GS shall be capable of sending user defined flight profiles to the aircraft**

Motivation: The aircraft needs to be able to be commanded, and in order to execute the full mission profile as described in the CONOPS, the command list must be uploaded to the aircraft avionics.

Verification: In testing for the aircraft's ability to execute the mission profile on a static test stand, the full command list will be uploaded and visually inspected till completion of the sequence needed.

- **DR 4.3: RC transmitter and receivers must be built in for emergency manual pilot control**

Motivation: The aircraft must be capable of being controlled from a pilot so that in an emergency landing in which the mission must be stopped, the aircraft may be commanded without crashing in that event.

Verification: In addition to commanding the aircraft while on a static test stand, hover controlled through only pilot input on the controller for flight shall be shown.

FR 5: The aircraft shall be capable of carrying a 0.5 kg payload.

Motivation: It is a customer request to support the addition of 0.5 kg which represents an available space in the mass budget for more scientific instruments/sensors.

Verification: The aircraft shall show this capability in analysis and upon completion of the aircraft, in a full mission profile flight test, from hover, loitering, landing and repeating that process.

- **DR 5.1: Aircraft is capable of lifting 0.5kg payload in vertical and horizontal flight modes.**

Motivation: Both aspects of the VTOL flight must be able to support the addition of the 0.5 kg payload in order to meet the requirement of including the additional capability.

Verification: Similar to the verification of FR 5, this requirement will be fulfilled with a full mission profile being executed with the extra mass. If the battery has sufficient charge left after the test, than it will be considered successful.

- **DR 5.2: Aircraft controllability accounts for presence of payload.**

Motivation: It is critical to the success of the project that the extra mass from the payload does noticeably impair the success of the mission profile completing and not greatly hinder the performance of the aircraft.

Verification: Using aerodynamic system data and modeling, show that the flight characteristics(controllability, modal behaviors) are still acceptable with and without the payload.

FR 6: Aircraft shall be capable of taking off from existing RAPCat launch system.

Motivation: It is a customer requirement that the VTOL aircraft still be capable of taking off from the existing RAPCat launch system. The RAPCat launch is a more efficient use of battery power than a vertical takeoff and will be used when available.

Verification: The aircraft will successfully mount and takeoff from the RAPCat system.

- **DR 6.1: Interface successfully with launch rail/tow hook after addition of VTOL components.**

Motivation: In order to facilitate a RAPCat launch the aircraft must interface with the RAP-Cat system.

Verification: The 3D model of the VTOL aircraft shall show the potential for integration with the rail and tow hook.

- **DR 6.2: Withstands 5G acceleration from RAP-Cat without plastic deformation of airframe.**

Motivation: The aircraft must be able to withstand the loading forces associated with the RAPCat launch.

Verification: A model of the aircraft under the predicted forces of launch will show no plastic deformation.

- **DR 6.3: Begin flight in level flight mode via RAPCat launch.**

Motivation: The aircraft must be able to enter steady, level, horizontal flight immediately after being launched by the RAPCat.

Verification: In a limited flight test, the aircraft will demonstrate the ability to take-off from the existing launch infrastructure after VTOL modifications are made.

- **DR 6.4: No modification of existing launch infrastructure.**

Motivation: In order maintain RAPCat functionality with the rest of the IRISS fleet, the RAPCat must not be modified for the VTOL aircraft.

Verification: Launch can successfully be completed without modification of the existing RAP-Cat system.

FR 7: The airframe, propulsion system, and required mounting hardware shall cost no more than \$1000 per aircraft.

Motivation: The customer's goal is to be able to manufacture individual units of the VTOL converted Drak at an economically feasible price of no more than \$1000. This budget does not include the provided avionics package as it is currently in use in other aircraft in IRISS' fleet and is already manufactured by them. This also does not include batteries as they already have purchased battery packs on hand and also have the capability to fabricate their own battery packs. The RiteWing Drak kit must be included in the unit cost as each time the VTOL aircraft is to be fabricated, a Drak kit must be purchased for modification.

Verification: An itemized budget will display each part along with the associated quantity and price for each to show the total single unit cost.

3.2 Propulsion

The Propulsion system operates with the goal to sustain self-sufficient force and power characteristics to maintain flight. For a VTOL aircraft, this includes high energy hover flight as well as lower energy level flight. In order to achieve this, four major components are seen below in Fig. 3 as well as final design components.

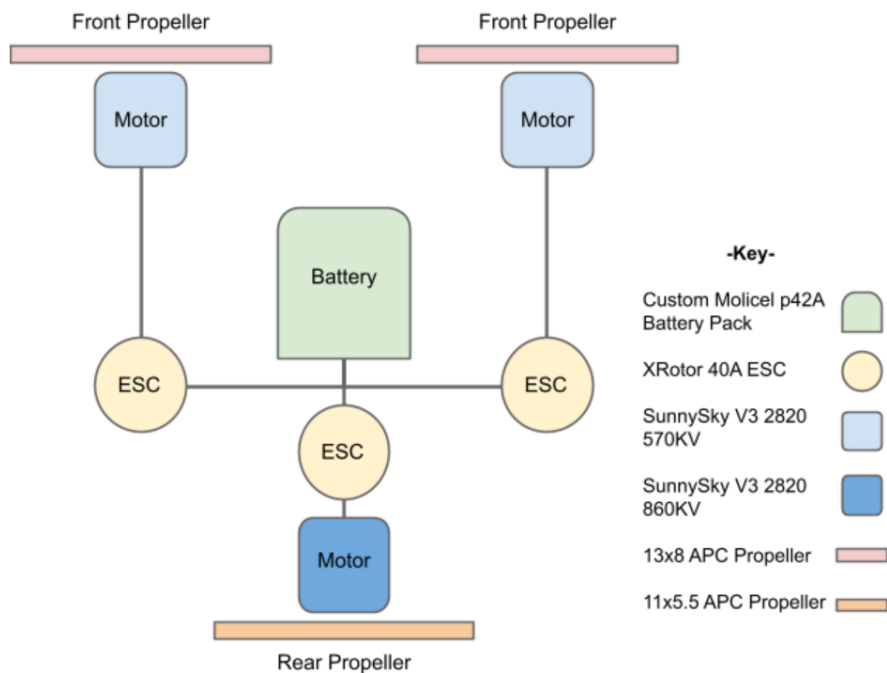


Figure 3: Propulsion Component Layout Diagram

- Propeller:** This component generates lift on the aircraft through momentum change and pressure distribution when in motion. Propellers are measured based on their diameter and pitch (twist). Each propeller has a desired angle of attack where the thrust to drag ratio is highest. Propellers were sized with the constraints of the aircraft center of gravity, tri-copter organization, and weight of the aircraft. The two front propellers were used for forward flight so high pitch sizes were needed for lower speeds (APC 13x8). The rear prop was only used in hover flight so a lower pitch propeller was selected (APC 11x5.5). The propulsion model was based on UIUC Aero-naut propeller database which allowed for realistic advanced ratios, efficiencies, and thrust coefficients. The accuracy of this model allowed for very optimized disc size and thrust performance in any flight condition.
- Motor:** This component is crucial in producing correct angular velocities (for thrust) with desired power inputs from the battery. After modeling many different brands and size motors, this VTOL aircraft used two SunnySky V3 2820 570KV motors for the front and one SunnySky V3 2820 860KV motor for the rear. These are high efficiency motors that allow

the aircraft to operate in high thrust situations as well as operate in low power cruise flight.

- **Electronic Speed controller (ESC):** This component simply controls the speed of the motor using integrated circuits. Internally, electromagnetic forces are manipulated (controlled by the flight controller) which allow a range of motor speeds required to fly the aircraft. This component is very common in RC aircraft and can be purchased off the shelf. The selected motors required a maximum of around 40A each to meet our modeled thrust requirements. The XRotor 40A ESC selected and used for all three motors, and maintained reasonable efficiency at a 6S voltage level with low weight.
- **Battery:** This power center of the aircraft. The battery is needed to maintain high energy density in order to output necessary current at a voltage level. When designing the battery for this aircraft, attention had to be made to two main battery characteristics: energy density and maximum current output. High energy density will allow for high endurance ((functional requirement 2). High current output will allow for high levels of thrust in takeoff and landing ((functional requirement 1). A trade study found Molicel 21700 P42A lithium ion battery cells to be sufficient. These cells were later optimized for custom battery design in order to better achieve project requirements. The final pack design is seen below in Fig. and is capable of 180A burst discharge, 16.8Ah capacity, Charged voltage of 25.2V. The optimal cell configuration was found to be 6 series and 4 parallel to best meet our requirements.

3.3 Structures

3.3.1 Requirements Flow Down

The primary requirements that the structures system addresses are requirement 1 as well as requirement 6 and its derivatives. Requirement 1 is a statement of the overall objective of the project: to convert the Drak airframe to accommodate vertical takeoff and landing. Requirement 6 comes from the desire for the customer to maintain their existing catapult launch capability. The aircraft needs to maintain ability to integrate into their RAPCat launch system as well as be able to withstand the acceleration of a catapult launch. The additional structure added to the Drak airframe enable VTOL flight using the tilting motors and extended rear motor. As will be seen forthcoming, many simulations were run to ensure the aircraft and all custom components could withstand all the forces seen during a typical flight regime including catapult launch, vertical takeoff, and a 10G landing the customer asked to design to.

3.3.2 Structures System Components

The rear motor mount is one of the essential elements that enables vertical flight. It hold the rear motor in a vertical configuration at all times. It attaches to the Drak's default motor mounting location and weighs 80 grams.

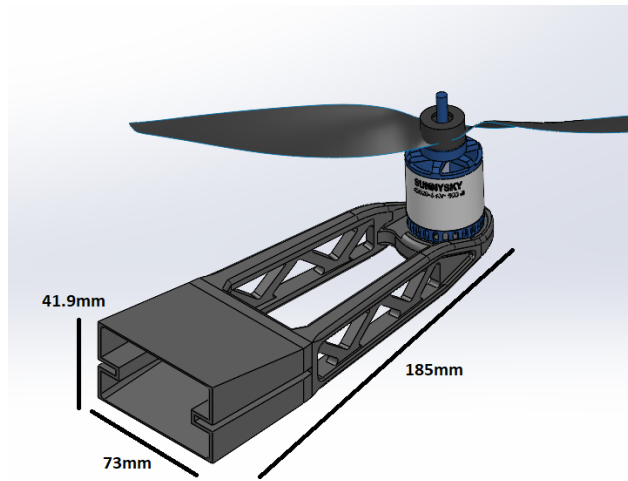


Figure 4: Design and Dimensions of the Rear Motor Mount

The main weight component within the structures system is the wing mounting motor arm assemblies. These hold the rotating motors mounted on the "saddle" pieces, as well as the servos used to rotate the motors.

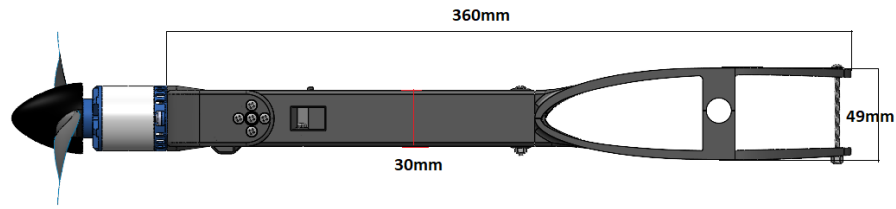


Figure 5: Front Motor Assembly with Dimensions

These components allow the Drak to be converted to a VTOL aircraft. The wing mounting motor arms hold the tilting motors which enable both horizontal and vertical flight (when used with the third, rear motor). This satisfies requirement 1, the VTOL conversion. All of these components were subjected to rigorous finite element analysis before finalizing the designs. The analyses confirmed that the parts could survive being subjected to the 5G RAPCat launch and 10G landing requirement. After verification testing, these parts did in fact meet this requirement and successfully launch from the catapult.

3.4

3.4.1 Controls

To actuate all of the control mechanisms, a Futaba SBUS receiver was provided by the client to connect to the avionics package pcb with the Futaba transmitter. Once the proper parameters for every servo output's function were defined on the groundstation software, then the transmitter could actuate each servo.

Two of the servos, HS-5065 models, were placed into a cut out on the wings and connected via a thin metal rod to a plastic pom horn on the ailerons. These servos were set as aileron servos to allow for 25 degrees of control surface throw for each wing. Limits on the PWM values that the

servos could take were defined to ensure that the servos were not pushing on the side of the cutouts, which could cause the teeth to break.

Two other servos, the HS-5065MG+ might feather model, were placed on the servo brackets on the tip of the wing motor mounts. These servos were meant to tilt the motors from a vertical position for hover mode to a horizontal position for level flight mode. These servos also had to go 20 degrees past the vertical to ensure yaw stability during hover mode since a tri-copter is inherently unstable in that configuration. Additionally, these tilting servos would add differential thrust capabilities during level flight mode. 20 degrees was set as the limit because any further than that would result in the propellers hitting the motor mounts. The controls actuation test showed that the servos were reaching all the required throws and at rate of 65 degrees per second, which is good for a fast transition.

The final servo, the HS-5065 model, was placed inside a cutout of the horizontal stabilizer. This is to ensure that the tail had proper pitch authority during level flight mode. The servo was also capable of reaching the required 25 degree control surface throw at a fast rate. With this test complete, functional requirement 3 is validated. Figure 6 shows some the PWM limits placed on each servo.



Figure 6: Controls Verification, PWM Limits Defined on GCS

As a final note, all of the servos were chosen to be digital servos, to ensure functionality with the provided avionics. Digital servos use the voltage given to them by the flight controller to stay rigid and not move at all during flight and whatever else. Analog servos are also easily move-able, are more sensitive to interference, and required re-calibration often.

3.4.2 Firmware

Functional requirement 3 is primarily satisfied by the flight controller firmware, ArduPilot. ArduPilot has robust control and navigation algorithms for both thrust-based and lift-based aircraft. The lift-based aircraft software (ArduPlane) is described here, but the thrust-based software (ArduCopter) is described in appendix B. Figure 7 outlines the ArduPlane parent loop. Completion of a mission profile without pilot input involves two major areas of interest. The aircraft must be stable and also must have adequate navigation characteristics. Stability is ensured by ArduPilot's attitude control algorithms, where PID control loops ensure adequate tracking of reference attitudes and rates. Sufficient flight path tracking is ensured by ArduPilot's navigation algorithms. An L1 controller uses a nonlinear guidance law to ensure that the aircraft follows the correct trajectory,

and a TECS controller uses PID control loops to ensure that the aircraft altitude and speed track the reference mission values. Both the stability and navigation functions require accurate state estimates, supplied by the Extended Kalman Filter. The EKF uses knowledge of system dynamics and sensor noise to accurately estimate the actual aircraft state. Other system functions account for pilot input and control input actuation. Functional Block Diagrams for the L1 and TECS controllers are given in Appendix B.

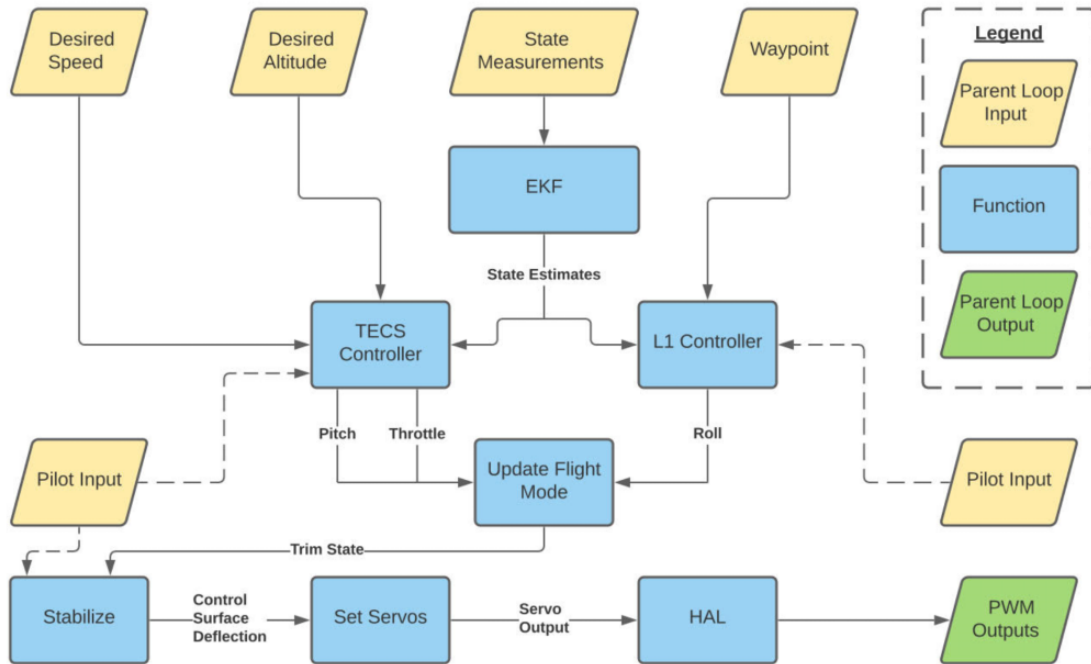


Figure 7: ArduPlane Parent Loop Functional Block Diagram

Traditional analysis of aircraft dynamics includes a few assumptions that often lead to imperfect control gain values. This includes neglecting the effect of spinning rotors, linearization of time-variant systems, inaccurate stability derivatives, and imperfect mass and inertia information. Thankfully, ArduPilot's "Autotune" function will tune gain values for the best aircraft performance. Figure 8 outlines the ArduCopter Autotune function. Through a series of "twitches," the function tunes gain values. The function invokes rate perturbations and attitude perturbations, and measures maximum rotation rate and "bounce back rate," or the attitude rate after overshooting the reference rate. The Autotune function adjusts the proportional and derivative gain values until the measured rates have the desired proportional relationship to the commanded rates. Integral gains are defined in proportion to proportional gains. There is an analogous Autotune function for the level flight mode, which is based off of pilot inputs instead of commanded twitches. In practice, the aircraft will first be supplied the calculated gain values, as a sufficient starting point. The autotuner will result in an aircraft that is stable in hover. This stable hover configuration will act

as the "bailout" mode during level flight tuning; if the aircraft loses stability while tuning the level flight gains, switching to the tuned hover mode will often prevent a crash. After the level flight tuner, the aircraft will be stable in both flight modes as well as transition.

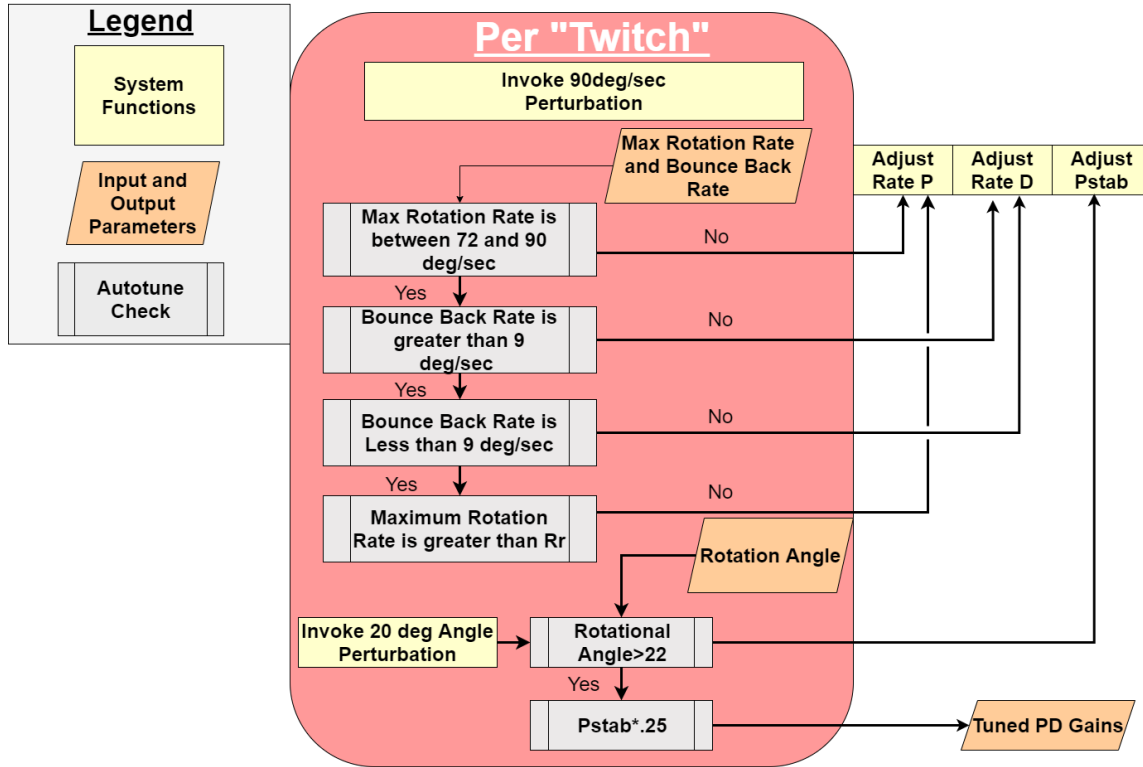


Figure 8: ArduCopter Autotune Functional Block Diagram

Design requirement 3.3 is one of particular concern, because accomplishing stable flight during transition is more complex than regular flight regimes. This is because the dynamics of the aircraft mid-transition are nonlinear and time-variant, meaning traditional PID control is not straightforward to implement. At a high level, these dynamics manifest themselves as a handful of challenges which the transition script is designed around handling. The primary challenge is that the script must "hand off" the controls from thrust-based commands to surface deflection based commands. During transition, the script cleverly prioritizes control outputs, such that redundant control outputs must be suppressed. For example, if both a front motor thrust command and elevon actuation would result in pitch actuation, one must be suppressed to achieve the desired result. The thrust-based command architecture (ArduCopter) is the active form of stabilization at low speeds, until the aircraft is moving fast enough that the control surfaces have adequate control authority. Another big challenge is the inherent coupling of control input responses while the motors are mid-tilt; differential thrust during the mid-tilt regime results in both a roll and a yaw response, while symmetric thrust results in both an airspeed and a climb response. This challenge is the most complex to handle, and Ardupilot handles it by commanding two control inputs that results in one out-

put. For example, during mid tilt, there exists a roll input command and yaw input command that, together, actually result in a pure roll. One final challenge that tiltrotor aircraft often face is insufficient lift-generation during transition. This is handled by limiting the thrust vector angle; Ardupilot ensures that the aircraft preserves climb capability given the **net** vertical force by limiting the angle that the rotors can tilt forward. Once sufficient lift is generate from the wing, the firmware allows the rotors to tilt fully forward. [47]

While Ardupilot has the capability to satisfy these design requirements, user-inputted parameters specify the exact, detailed values that will tell the firmware how to command and control our specific flight configuration. There are a few groups of parameters that work together to define specific portions of the aircraft configuration. Plane parameters involve defining servo details and purposes, defining RC input properties, defining the rangefinder properties, and defining flight characteristics such as maximum climb rate or failsafe characteristics. QuadPlane parameters involve configuring the VTOL aspects of the aircraft and mission profile. This includes defining the tri-copter frame and tiltable rotors, but also includes defining the desired behavior of the aircraft during takeoff, landing, and transition. Finally, both plane and QuadPlane have many tuning parameters, for both the stability and navigation controllers. Some of these parameters come from dynamic analysis and Autotune, while other parameters depend on physical aspects of the aircraft, such as propeller size and motor/ESC combinations.

3.5 Autonomous Flight

The automated missions can be created from the graphic user interface(GUI) that ArduPilot provides, called MissionPlanner. This GUI is the interface that allows for flashing firmware, editing parameters, programming extra hardware (LiDAR), and planning autonomous missions. The autonomous aspect of the firmware can only be tested once the aircraft has proven to be stable in both flight regimes, as pilot input will not be able to correct for a possible issue in the gains or parameters. Prior to stability being shown, a variety of autonomous missions could be created in MissionPlanner. The most important flights for showing autonomous function were:

1. Takeoff - Hover - Land
2. Takeoff - transition - loiter - transition land
3. Full Mission Profile: 2 - takeoff and landings with 30 min loiter between

Before any of these missions were attempted, the parameters of ArduPilot must be reviewed to choose the characteristics of autonomous behavior. A few features not previously discussed could be changed at that point, such as loitering in VTOL versus forward flight, enabling GeoFences, and enabling VTOL lift assistance. Loitering in VTOL versus hover is important to show the different aspects of the aircraft, as our main mission profile includes loitering in forward flight for half an hour, while our first important flight includes a VTOL loiter to demonstrate stability in the hover mode. GeoFencing is a feature in ArduPilot & Mission Planner in which a boundary can be programmed into the flight controller prior to a piloted flight. The boundary can be drawn on a map in the GUI, seen in red on figure 9, and is a flight safety feature required from the Flight Director of CU, Dan Hesselius, that essentially limits the plane to those boundaries. If the pilot flies the plane outside of the red fence, the plane will go into an autonomous guided mode that takes the

aircraft back to the launch location. Lastly, VTOL lift assistance is a feature that allows for the motors to tilt slightly vertical to provide extra lift when below certain speeds. This was important safety feature early on in the project, as unsure lift results were found from the aerodynamic test stand, but this was later found to not be necessary due to the flight characteristics in forward flight, later discussed in this paper.

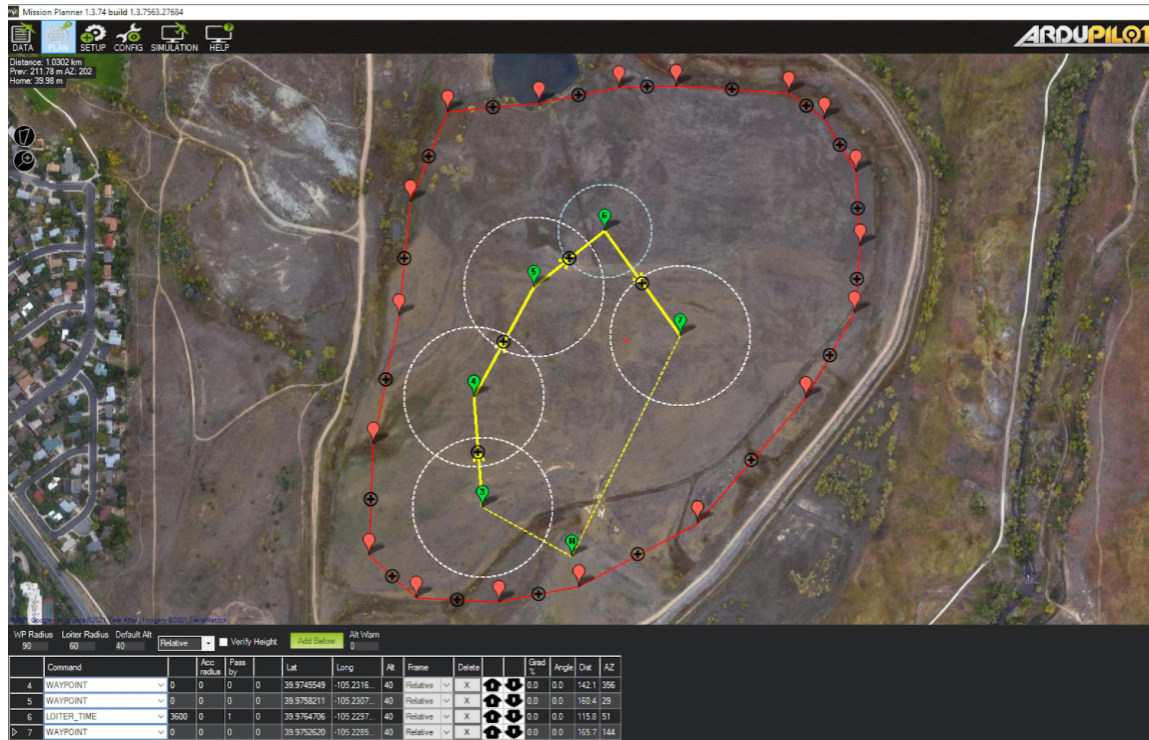


Figure 9: Mission Planner forward flight loiter test.

With desired flight features identified, the test flights could then be created in Mission Planner. All were planned with a series of DO commands, seen as actions, in the bottom command window of the test flight mission seen in figure 9. The first test flight is a planned simple hover and loiter in VTOL mode, to evaluate the autonomous hover ability of the aircraft and prove stability through takeoff and landing. The test that is seen in figure 9 is the forward transition and loiter test, which was planned to prove that the aircraft can autonomously transition in and out of forward flight, and to give confidence that the loiter will perform as expected during a full mission profile. Finally, the full mission profile flight test was to validate the endurance requirement of the VORTEX aircraft and verify the integrity of the system design over a long window. Mission Planner allows for each action to have input parameters specific to it, such as loiter time and radius for all loiter actions, altitude for all waypoint actions, or commanding the aircraft in or out of forward flight to control transition.

3.5.1 Avionics

Talk about ardupilot quadplane, discuss major components configured (frame, servo functions, lidar, battery monitor, ESCs maybe), discuss mission planning and maybe autonomous behavior (ie waypoint response, transition times, flight modes in use, etc).

Prior to making any design changes to the avionics system, it was crucial to fully understand the function of the avionics package that was provided to the team by the customer. This includes a red printed circuit board, which integrates nearly all peripherals and other components. The battery pack provides power to both the electronic speed controllers and to the red PCB directly via a power module, also provided by the customer. Voltage regulators on the PCB step the voltage down to 12V and 5V. The custom telemetry package provided by the customer, which is the only peripheral powered by 12V, is used to send aircraft and sensor information back to the ground station. All other peripherals are powered by 5V, including the Hex Cube Black flight controller, which is responsible for autonomous flight. It assists in manual flight as well. While in manual flight, the SBUS receiver relays commands from the pilot to the flight controller, which performs certain calculations based on the parameters set in Mission Planner that have been flashed to Cube and its internal IMU's. It then passes these "enhanced" commands to the respective recipient, e.g. an ESC or motor servo. Another peripheral critical for autonomous flight is the GPS navigation module, connected to the PCB via a telemetry port. This module communicates with the flight controller as well as relays aircraft position information to the ground station. Autonomous mission profiles are not possible without the GPS. Figure 10 below shows the custom avionics package and LiDAR partially assembled with the Drak fuselage/

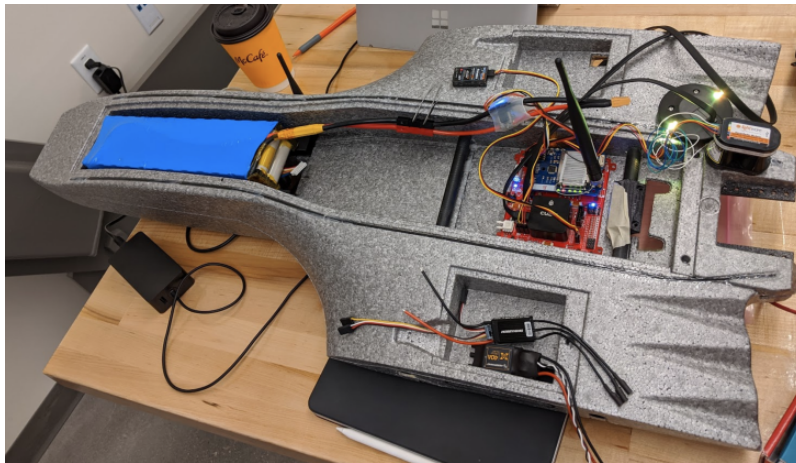


Figure 10: Avionics

Perhaps the most critical design modification to the avionics system was the addition of the front tilting motors. Each of the front tilting motors requires a servo motor, electronic speed controller, and motor. The servo motor is used to tilt the motor system between vertical and horizontal orientations during flight mode transitions, and is responsible for yaw control as previously discussed. Servo deflection, which is responsible for tilting the front motors, is controlled and powered via the pulse width modulation ports on the avionics board. The electronic speed controllers govern the

propeller spin rate of the front motors, which is set to be equal but opposite to provide moment stability. A critical preflight check is to ensure the correct spin direction of these front motors.

The addition of the rangefinding LiDAR was critical for obtaining accurate altitude data, which allowed for gentle vertical landings. The LiDAR was configured as the primary source of altitude data within Mission Planner for the desired range of altitude, which was set from 0 to 40 meters. The LiDAR communicates with the red PCB via a UART connection.

3.6 Aerodynamics

The aerodynamics design was primarily focused on the horizontal flight condition, since the flight condition in cruise would determine whether the endurance requirement could be satisfied.

3.6.1 Flight Characteristics Estimation

The estimation for lift and drag started with estimation of the lift characteristics using Prandtl Lifting Line Theory, using MATLAB code developed primarily from prior aerospace classes. SolidWorks was chosen for ease of use in rapid iterations for testing different flight conditions. First, the unmodified Drak was tested at a variety of angles of attack to get the drag polar. The same was repeated at different points throughout the design process, with the VORTEX/No Tail being the model made after CDR. The final design is the VORTEX/Tail which includes the most up to date version of the design at time of writing.

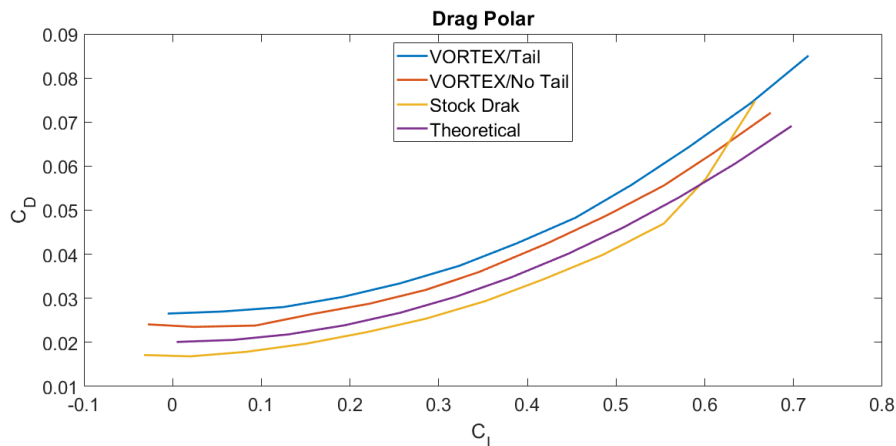


Figure 11: Drag Polar

3.6.2 Tail Design

The primary motivation for the tail design was the results of the CFD simulation performed at the end of fall semester. Those simulations were done with the intention of finding the deflection of the elevons that would zero out the moment induced on the aircraft. The problem was that when the aircraft was at an AoA where the lift cancelled out the weight, there was a nose down moment which needed to be countered by pitching the elevons up, which in turn reduced lift. This effect pushed the cruise condition to a higher angle of attack, which was too close to stall for the team's

comfort. To counteract this, the team opted to add an empennage to increase lift and shift the trim condition away from stall to a lower AoA. The options considered for this empennage were either canards at the front or a tail at the rear of the airframe.

Due to the heritage of the RAAVEN tail and the additional structural and stability concerns of using canards, the decision was made to begin making the tail. The base design is based on the RAAVEN tail, using two Coroplast booms with a similar shape to the RAAVEN tail and a foam airfoil for the horizontal stabilizer. The last 0.05 m of chord of the airfoil is cut off and taped to the back to act as an elevator. A single servo is embedded into the center of the horizontal stabilizer and used to control the elevator.

Sizing of the horizontal stabilizer was determined starting from the standard longitudinal stability equations for a conventional aircraft. Four equations were used in the first steps of the derivation: force equilibrium in trim, moment equilibrium in trim, static stability, and static margin. Using the FBD below, the equations were derived for the quantities as labeled.

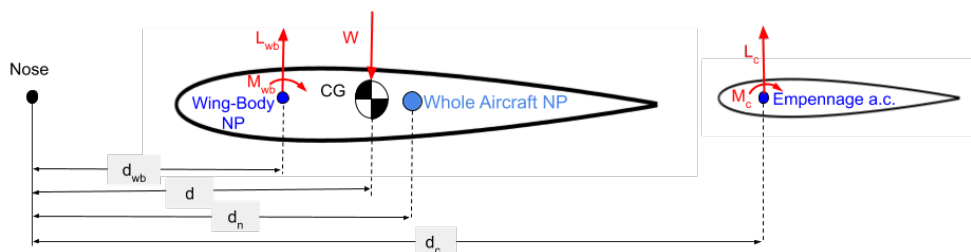


Figure 12: FBD For Tail Design

$$\begin{aligned} \frac{W}{q_\infty} - SC_{Lw} &= C_{Lc}S_c && \text{Force Equilibrium} \\ \frac{Wd_{wb} - M_{wbac}}{q_\infty} &= -d_{wb}C_{Lc}S_c + C_{Lc}S_cd_c + \frac{Wd}{q_\infty} && \text{Moment Equilibrium} \\ d_n &= \frac{C_{Lc\alpha} \frac{S_c}{S} d_c + C_{Lwb\alpha} d_{wb}}{C_{Lc\alpha} \frac{S_c}{S} + C_{Lwb\alpha}} && \text{Static Stability} \\ K &= d_n - d && \text{Static Margin} \end{aligned}$$

From these initial equations, we derived a set of four equations that would determine positioning and sizing of the tail. Of these equations, three could be arranged into a matrix system of equations, which was solvable once the remaining equation was solved. The output is the planform area of the horizontal stabilizer, the distance from the nose of the tail, neutral point and the center of mass based on the desired static margin.

$$S_c = \left[\frac{a_{0c}(\alpha - \alpha_{L=0})}{\frac{W}{q} - SC_{Lw}} - \frac{57.3a_{0c}}{\pi e c b^2} \right]^{-1}$$

$$\begin{bmatrix} \frac{Wd_{wb} - M_{wb_{ac}}}{q} + d_{wb}C_{LC}S_c \\ -C_{Lwb\alpha}d_{wb} \\ K \end{bmatrix} = \begin{bmatrix} C_{LC}S_c & 0 & \frac{W}{q} \\ C_{LC\alpha}\frac{S_c}{S} & -[C_{LC\alpha}\frac{S_c}{S} + C_{Lwb\alpha}] & 0 \\ 0 & 1 & -1 \end{bmatrix} \begin{bmatrix} d_c \\ d_n \\ d \end{bmatrix}$$

In order to rapidly iterate and keep track of the many variables involved in the design process, a custom MATLAB GUI was developed. The GUI tracks environmental conditions, variables related to the airframe, the airfoil for the tail and the actual sizing and position of the tail.

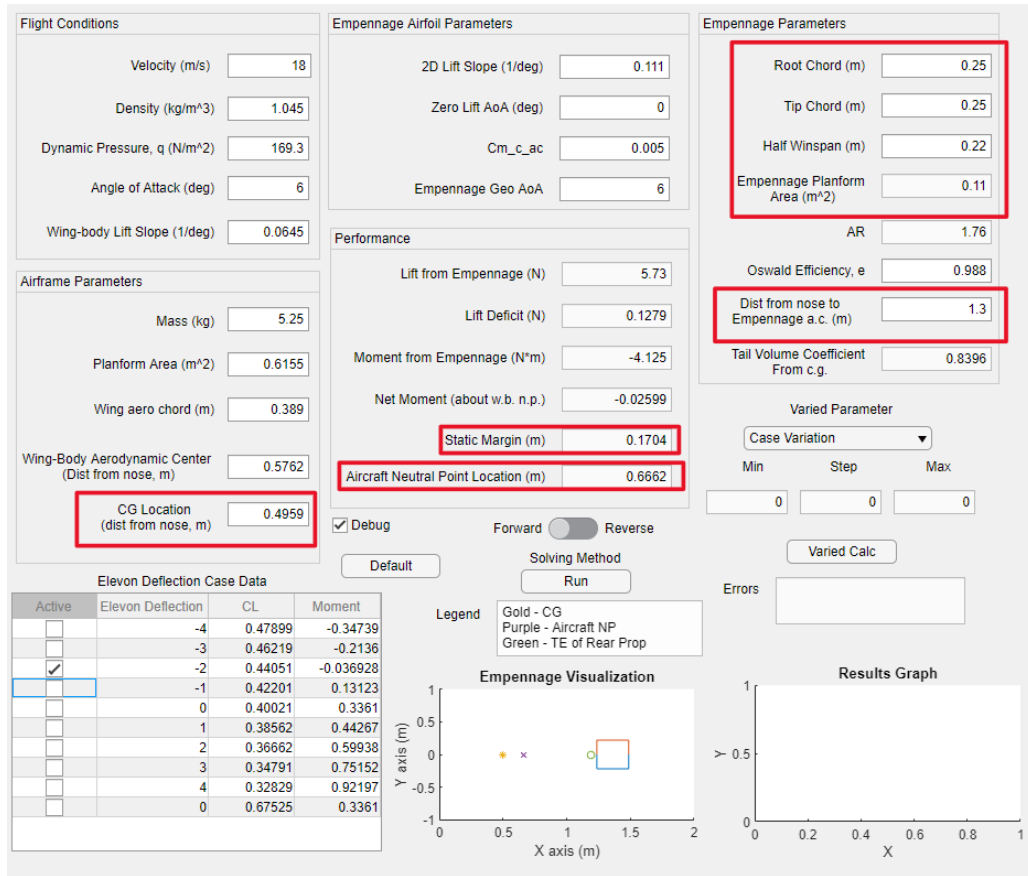


Figure 13: Tail Design GUI

The GUI picture here shows the parameters for the final design parameters, highlighted are the primary parameters of interest for the design phase.

For sizing the vertical stabilizers on the tail boom, the equation in [50] was used for calculating the needed vertical volume coefficient to achieve static stability in yaw. The decision to focus primarily on yaw came from the lack of yaw control surfaces and the roll authority granted by repurposing the elevons as ailerons.

$$C_{N\beta} = \frac{2S_{Fl}F a_c}{Sb} \left(\frac{V_f}{V} \right)^2 \left(1 - \frac{\partial \sigma}{\partial \beta} \right)$$

The final decided size for the vertical tail was 0.03239 m^2 per vertical tail segment.

4 Manufacturing

Section Authors: Brandon Cummings, Colton Cline, Joseph Rooney, Stephen Albert, Joseph Buescher

Component	Amount	Source
Avionics Package	2	Provided
Drak Wing Kit	3	Purchased
Motor Mounts	2	Manufactured
Empennage	3	Manufactured
Batteries	2	Manufactured
Integration, Wiring, Gluing	N/A	Manufactured
Test stands	2	Manufactured
Miscellaneous	N/A	Manufactured

Table 2: Overview of Manufacturing

4.1 Stock Drak Body

In order to satisfy the first functional requirement FR1 and begin manufacturing, all modifications had to be made to the COTS RiteWing Drak kit. All of the components that can be found in one of these kits have been put into Table 3 and can be seen in Figure 14. Three of these wing kits were purchased as well as an extra set of wings as a precaution for any accidents and failed flight tests. The owner of RiteWing has an assembly video detailing the assembly process for the stock Drak that was slightly modified to fit the needs of this project. A brief description of the assembly process can be found later in this section.

Component	Quantity	Component	Quantity
Fuselage	1	Carbon Fiber Sleeves	2
Vertical stabilizers	2	Spar Channel Plugs	6
Winglets	2	Rear Motor Mount	1
Payload Covers	4	Rear Motor Mount Cap	1
Left Wing	1	Plastic Lamination	1
Left Elevon	1	Plastic Black Screws	8
Right Wing	1	Metal Hex Screw Cones	8
Right Elevon	1	Small Hex Bolts	4
Carbon Fiber Spars	2	Small Nuts	4
Carbon Fiber Rods	18	Small Washers	4

Table 3: Base Drak Wing Kit Components



Figure 14: Base Drak Components

4.2 Motor Mounts

The bulk of the weight that was added to the aircraft was in the 3D printed motor mounts that enabled VTOL functionality. These were 3D printed using PETG filament, which was chosen because of its rigidity and resistance to weather degradation. Manufactured 3D printed parts included two wing mounted motor arms, the two halves of the clamping motor arm mount, the rotating motor "saddle", and the rear motor mount. The convenience of 3D printing fit excellently within COVID-19 guidelines. Two of our team members own personal 3D printers which enabled the team to continue production no matter the state of lockdown restrictions.



(a) Layer Shifting on a 3D Print



(b) Successful Rear Motor Mount Print

The teammates with 3D printers managed the division of labor for producing these parts. The challenges faced when manufacturing our 3D printed parts were the usual problems that 3D printers face. After adjusting settings (temperature, print speed, retraction) specific for PETG, there needed to be further tuning when specific problems were encountered. For example, one print of a motor arm experienced layer shifting, which is when layers of filament do not properly stack on top of one another throughout a print. This is an unpredictable problem which can come about anytime a part does not adhere properly to the print bed or it can be caused by low voltages to stepper motors controlling the extrusion head positioning. For our team, this was a one time error that resolved itself after resetting the printer. Over time, printing became more consistent and parts had better layer qualities and tolerances.

Figure 16 displays the Solidworks CAD model of the assembled motor arm, which mounts on the wing. This image includes the two halves of the bracket, motor arm, and saddle, on which the motor attaches. This assembly was mounted on the plane along with the rear motor mount successfully, as seen in Figure 17.

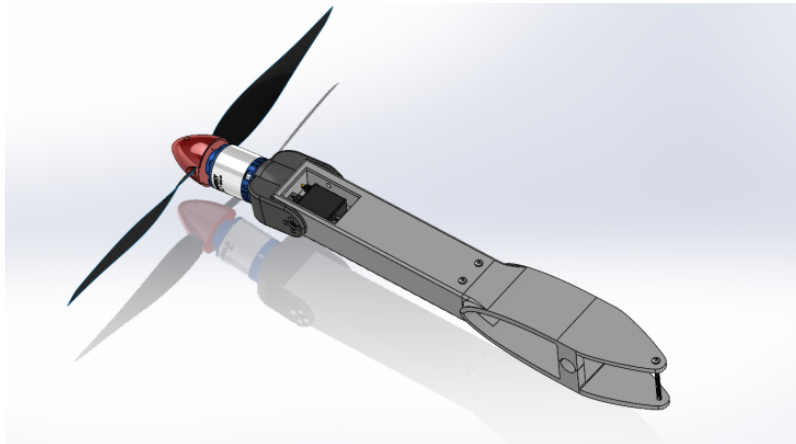


Figure 16: Rendering of the full motor arm assembly



Figure 17: Fully Assembled VORTEX aircraft

4.3 Empennage

The manufacturing of the empennage was strongly influenced by the tails that are currently used with the IRISS UAS, as they provided a working prototype that could be improved upon. It was found that their purchased tail was heavier than the VORTEX team could operate with, so

Component	Source
Coroplast Stabilizers	Designed and Ordered
EPP Foam Airfoil	Manufactured
Servo and Wire	Purchased
Laminate Film	Supplied by RightWing

Table 4: Tail Manufacturing Overview

inspections were made to reduce mass, while prioritizing strength and stability. Upon evaluation, the team found that the EPP used was too dense, the wood used for the tail’s elevator was unnecessary, the servo used for the elevator actuation was too-large and oversized for the task, and finally the carbon fiber spars through the Coroplast vertical stabilizers were found to be both unnecessary with thick enough Coroplast and outside of the project budget.

In manufacturing the VORTEX tail, the design for the vertical stabilizers, previously discussed, was cut out of 10mm thick CoroPlast using a CNC router at PlastiCare Inc. From this point, the airfoil cutout discussed earlier was manufactured using a manual hot wire cutter from the AERO Electronics shop. First, an EPP foam with less density than the RAVEN tail was used for the airfoil cutout. With the airfoil cutout, the elevator was cut out from the back side of the already shaped airfoil, instead of using a wood piece. It was determined that the servos already used in the project for the ailerons had more than enough torque to fully actuate the elevator on the tail, which also meant no extra hardware had to be ordered. With the smaller servo selected, a cutout was made on the surface of the airfoil to accommodate it.

With the servo in place, all of the components of the tail were in place to be assembled. The process began with wiring the PWM cable extension through the Coroplast tail, leaving just enough wire hanging through the airfoil cutout on the vertical stabilizers to reach the elevator servo. With the wiring done, the foam airfoil with the servo could be mounted into the stabilizers. First the airfoil is fit, then hot glue is added on both sides where the airfoil is fit through the cutout. With the airfoil fit, the cable was routed to the servo, making sure to keep it as taut and close to the surface of the airfoil as possible. At this point, both of the foam pieces were then individually wrapped in a laminating film that was included in the original DRAK wing kit. The laminating film adds another layer of strength to the foam cutouts and reduces the parasitic drag of the tail as it covers the rough skin that results from a hot wire cutter with EPP. With the airfoil laminated and mounted, the elevator was taped on using high strength clear tape in a similar fashion to the DRAK aileron mounting, crossing tape from the bottom to the top and vice-versa. Finally the control horns and rods were connected to the servo and the 3-D printed landing skids were attached to complete the tail.

4.4 Batteries

A battery pack was manufactured in order to have both flexibility and optimized performance. Battery packs purchased off the shelf become expensive, heavy, and limited for our purposes in creating a VTOL aircraft. The decision to purchase individual cells and construct a battery pack saved on cost, but ultimately allowed for better optimization in structure, configuration, and performance. Comparing our model with vendor data and independent forums, a lithium ion cell was

chosen (Molicel p42A) in the configuration of six series four parallel (24 cells). All components were purchased separately and assembled at one time. This included insulation rings (for additional safety), cell brackets (for structure and ease of manufacturing), nickel strips (for welding cells together), Kapton tape (insulation), balance charging plug, and additional wire/plugs needed for leads and charging. With careful planning and attention to specifications, a design layout for manufacturing (12x2) is seen in Figure 18. A spot welder (from IRISS) and soldering iron were used to assemble the battery with proper safety precautions. The final battery is concealed in shrink wrap as seen below.



Figure 18: Battery Manufacturing

The assembled battery requires a relatively sophisticated battery charger to properly balance and monitor each cell during charge (therefore a battery management system was not used). Additionally, in-flight voltage can be easily read by the pilot to prevent unsafe discharge. The outcome of this manufacturing was two successful battery packs. The original design was not altered due to the sufficient performance of the first battery pack. With some flight crashes, high impact landings and long duration hover flights, the battery cells and manufactured pack proved to work robustly as designed. Few challenges were encountered. Additionally, structured battery brackets are strongly recommended for easier manufacturing. This component is easily integrated into the full system and secured into the fuselage with velcro. A XT90 plug connects positive and negative terminals into the power module for onboard electronics.

4.5 Test Stands

4.5.1 Static Test Stand

The design of the static test stand was based off of the stand the Design Build Fly (DBF) club lent to us. The stand came with several notable safety issues such as cracked or chipped protective panels, no screen to catch a detached propeller, and insufficient weight which caused it to be blown back if not held down. The new stand was built with these safety issues in mind. The stand can be seen below in Figure 5.2.1.

The stand is constructed with metric 30mm x 30mm aluminium extrusion and is held together by 64 90° brackets fastened with T-nuts. There is a screen attached to the front of the stand to catch a loose propeller and an $\frac{1}{8}$ in thick acrylic on the two sides and roof to protect from propellers that fail catastrophically while remaining visible for observation. The motor mount, RCBenchmark board, and load-cells were lent by DBF.

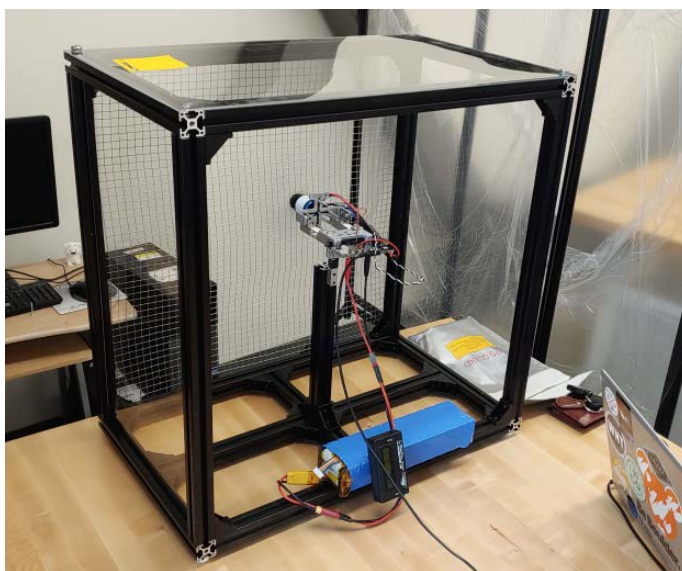


Figure 19: Static Test Stand

4.5.2 Aerodynamic Car Top Test Stand

The design for this stand drew inspiration from the desire for lift and drag data and the knowledge that the stand would have to interface with the roof rack of a vehicle which ideally wouldn't be affected by the dynamic air flow surrounding a modern car. In order to move away from the turbulent airflow above the car as much as possible, a requirement was made that the aircraft must be raised at least 1m from the top surface of the vehicle. Due to the large moment arm caused by applying forces 1m from the mounting point, this raised the need for the stand to focus on a high strength to weight ratio, while keeping in mind manufacturing and assembling constraints to the project. In order to make a stand that would meet both of those goals, a standard square aluminum extrusion was chosen to be the material that would make up the majority of the structure. The group settled for a 30mm x 30mm V-channel extrusion, which is wide enough to provide the rigidity needed, can utilize T-nuts for easy assembly, and is easy to manufacture, as aluminum allows for easy cutting. The test vehicle was selected early in the process so that the base of the stand could be cut to the proper width such that the side pieces would be aligned with the vehicle's roof rack rails. Simple steel U-bolts were used to provide the rigid interface between the stand and the roof rack rails. The test stand can be seen below in Figure 20. After the initial design of the base and car-stand interface was decided, attention was shifted to the data capture mechanism. Since we knew that load cells would have to be used, it was pertinent to make a configuration of cells that would structurally provide the support needed to the aircraft, and would report reasonably reliable data. It was decided that the cells must be in the L-configuration, as seen in Figure 21, in order to facilitate measurements of lift and drag forces on the Drak. Having the two cells at a right angle from one another provides the data for lift and drag as shown later. Summing together the corresponding data in the forward and upwards direction would provide useful insight to the forces the aircraft is experiencing. Since the L-shape was a chosen, the interfacing brackets had to



Figure 20: Aerodynamic Test Stand

be designed for an interface of the aluminum to drag load cell, drag load cell to lift load cell, and lift load cell to the rod that will connect to the mount inside the aircraft. Interfacing components were designed to be printed with Taulman Nylon Alloy 3-D printing material and were made to do both the interfacing from the aluminum to the load cell and from the lift load cell to the carbon fiber rod; this whole assembly can be seen in Figure 21. To ensure that data could be obtained at various angles of attack, a sliding bracket was designed for the front interface of the test stand. This sliding bracket is attached by inserting the mount into an opening in the underside of the aircraft and securing it in place with another carbon fiber rod, as shown in Figure 21. This would allow the front of the plane to shift up and down for different angles of attack as desired by sliding the 30mm x 30mm aluminum extrusion in the front arm of the stand.

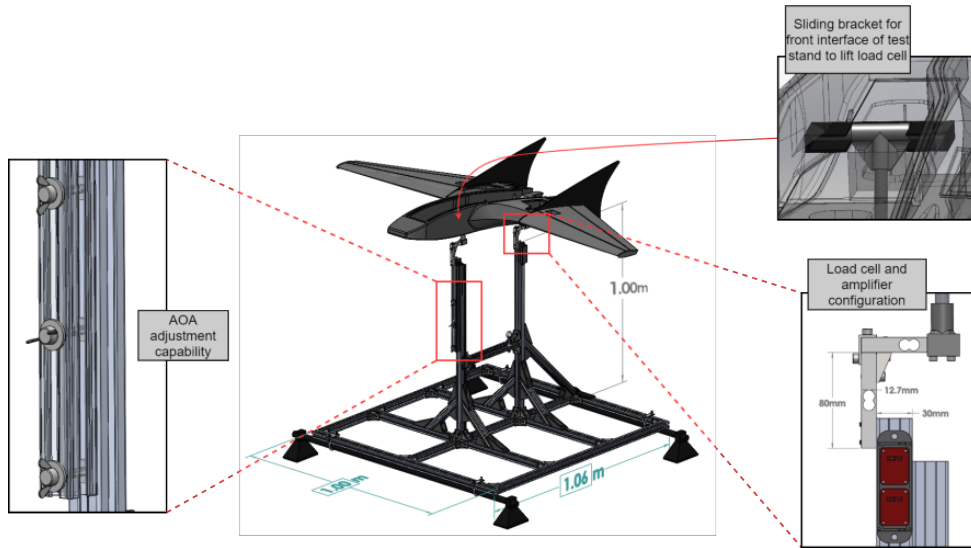
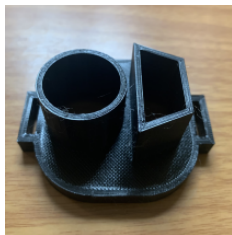


Figure 21: Aerodynamic Test Stand Interfaces

4.6 Other Manufactured Components

There were a few smaller components that require discussion as well, namely the LiDAR bracket and the RAPCAT hook.

The LiDAR sensor, the LeddarOne manufactured by LeddarTech, is a distance measurement sensor that was required to add accuracy during landings and takeoffs. The given sensor package that includes a barometer, gps, and compass is adequate but a LiDAR was supplemented to add accuracy during harsh weather conditions and uneven ground conditions. It however lacks proper casing for protection so to ensure that it remains safe during missions, a bracket was 3D printed and placed into a hole cut into the fuselage of the UAS. Figure ?? shows the sensor in the UAS, the bracket, and the modified bracket using the LiDAR test.



(a) Base LiDAR Mount



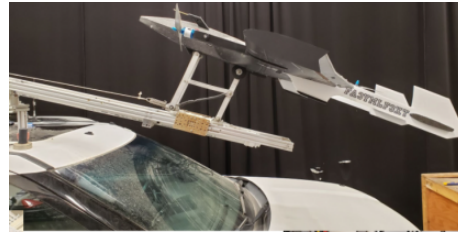
(b) LiDAR Mount for Testing

Figure 22: Manufactured LiDAR Mounts

Moving on to the RAPCat hook, One of the client requirements were that the UAS must be compatible with their existing RAPCat launch system, which is a pneumatic launcher used for all their other UAS systems. A RAPCat hook that interfaces with the RAPCat launcher was 3D-printed and incorporated into the bottom of the fuselage near the nose of the plane. Figure 23b shows the system fitting on to the RAPCat launcher and the manufactured hook.



(a) RAPCat Hook



(b) RAPCat Integration

Figure 23: RAPCat System

4.7 Assembly and Integration

The assembly process for the modified aircraft only has a few extra steps when compared to the assembly of the base Drak wing kit. A brief description of the modified assembly process highlighting major differences is given below.

Starting with the COTS base Drak wing kit, the filler ports were removed from the underside of the fuselage and wings. Next, all the surfaces that will be in contact with glue were sanded. Using the 3D printed wing mounts, the bottom mounts were placed in the spar channel on the underside of the wings. The wing mount was designed to be 15cm from the root of the wing. Both sides of the wing mount were marked in the spar channel with a pen and the mount was then removed. The marked rectangle in the spar channel was cut out using a sharp knife. An example of the hole can be seen in Figure 24a. The remaining procedures were similar to the base Drak assembly. The spar sleeves were glued into the wings and fuselage, making sure that they were straight and in line with each other. Next, the spar channel caps were glued into their respective locations. The rear motor bracket and rear motor cap were then glued to the fuselage. The smaller carbon fiber rods were cut to size and glued into their respective channels on the outside of the fuselage and wings.

With the majority of airframe now assembled, a 3D printed bracket used to hold the avionics board was glued into the fuselage between the spar sleeves. On the underside of the aircraft towards the nose, the 3D printed RAPCat bracket was installed using hot glue and two screws that attached to a second bracket located inside the fuselage. A pitot probe was also installed on the top left side of the airframe. Next, wire channels were carved in and between the fuselage and the wings using a hot wire foam cutter. The 3D printed rear motor mount was slotted onto the rear bracket and glued into place with hot glue. The rear motor was then screwed into the mount and the wires were routed into the fuselage.

To finish assembly of the wings, the aileron servos were screwed into the 3D printed servo housing and the housings were glued into the respective indentations located on the top of the wing. A



(a) Wing Mount Hole



(b) Early Version of an Assembled Wing

Figure 24: Aircraft Wings Along Assembly Process

control rod was then cut to size and connected the servo arms to the control horns on the ailerons. Next the 3D printed wing mounts were installed onto the wings. The forward motors were screwed into the 3D printed motor saddle. The motor and saddle attach to the 3D printed motor arm at two points. One side of the motor saddle uses a ball bearing for smoother rotation and the other side connects a servo that is mounted in the front of the motor arm. With the motor, saddle, and arm all connected, the servo and motor wires are routed through the motor arm. The wires then travel between the wing mounts, through the leading edge of the wing, to the root where the wires enter the fuselage. The motor arm is slotted over the wing mounts and secured together using two vertical screws. An example of an early version of the assembled wing can be seen in Figure 24b.

To complete assembly of the aircraft, the fuselage and empennage were aligned and the two carbon fiber spars were inserted. The wings were partially installed on the spars, wires were routed into the fuselage, and then the wings were installed completely. The wings were held onto the spars and fuselage using Velcro straps on the underside of the aircraft. The avionics board was then inserted to the bracket mentioned earlier and screwed into place. The motor wires connected to the ESCs located in the sides of the fuselage. All of the servo and ESC signal wires, eight in total, connect to the avionics board. The board and all other electronic systems were powered by the custom manufactured battery that was housed in the nose of the fuselage. The battery was secured in place using Velcro strips and was used to adjust the aircraft's center of gravity as needed. A fully assembled aircraft example can be seen below in Figure 25.

5 Verification and Validation

Section Authors: Brandon Cummings, Roland Ilyes, Joseph Rooney, Colton Cline, Mohamed Aichiouene, Justin Troche, Bill Chabot

5.1 Wing Motor Arm Stress Testing

To ensure the wing mounted motor arms could withstand the forces seen during a typical flight regime, they were subjected to tests which incrementally increased the force on the end of the arm. These tests verified functional requirement 6.2 and confirmed that the Finite Element Analysis



Figure 25: Assembled Aircraft

performed earlier in the design phases of the project was accurate. To perform this test, a spring scale and bucket were hung from the end of the motor arm, to which small weight was added in 0.5kg increments. This weight simulated the forces seen on the motor arms during vertical flight, the most strenuous flight mode. The motor arm was tested to weights of 2.3kg in a landing configuration and 6.3 kg in a takeoff configuration. The 6.3kg test sufficiently exceeded the needs of the design requirements with a large factor of safety. This verified that the motor arm could meet the needs of the project.

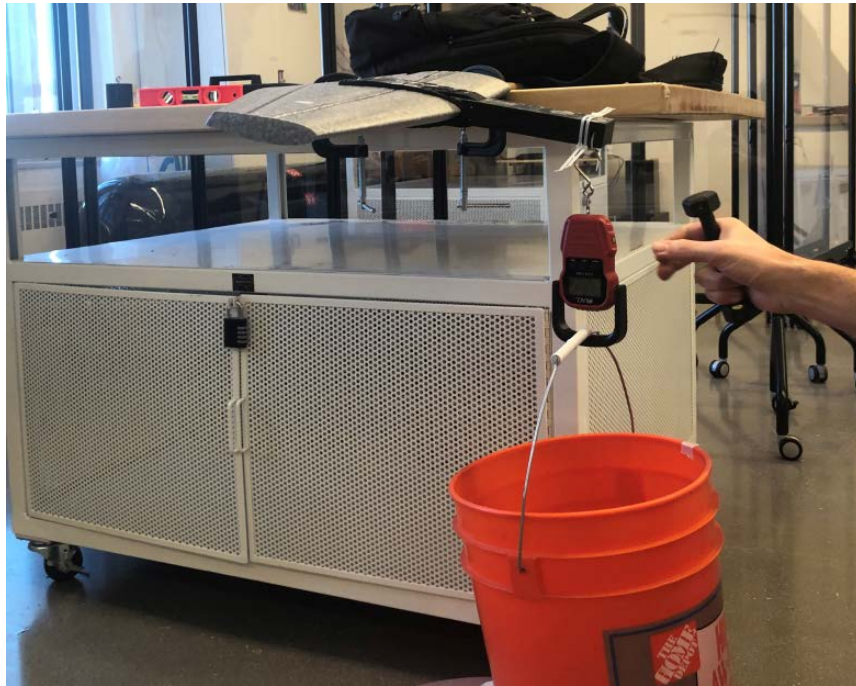


Figure 26: Motor Arm Stress Testing

The testing setup can be seen in figure 26, which was taken during an in-progress stress test. This picture was taken near the maximum stress exerted on the motor arm. An important observation taken during the test was the deflection seen in the wing when this weight was carried by the arm. There is extreme deflection in the wing holding the arm at this weight, but neither the arm nor the wing experienced any plastic deformation. The motor arm out performed its expectations and maintained more weight than that of the entire aircraft.



Figure 27: Rear Motor Mount Stress Testing

The same test was conducted for the rear motor mount with a slightly different setup, pulling upwards instead of downwards. Figure 27 shows the testing setup as well as the deflection in the rear mount. The 7kg weight exceeds the 3kg requirement giving a FOS of 2.33. The slight deflection did not cause any plastic deformation.

5.2 Battery Endurance

5.2.1 Static Endurance Test

Initial battery endurance was conducted by simply running the battery at a desired current and monitoring voltage drop off. This was conducted using the static test stand and RC benchmark software. A battery endurance test was necessary to compare to our modeled performance in order to mitigate performance shortcomings. Simply, the motor and propeller were configured exactly like a regular static motor test, but the test was run until the charged battery became discharged (See Fig.). The RC benchmark software tracks different parameters such as voltage, current output, and power while separate measurements were taken on a power module to record Ah discharge. These results can be seen below in Fig. 28

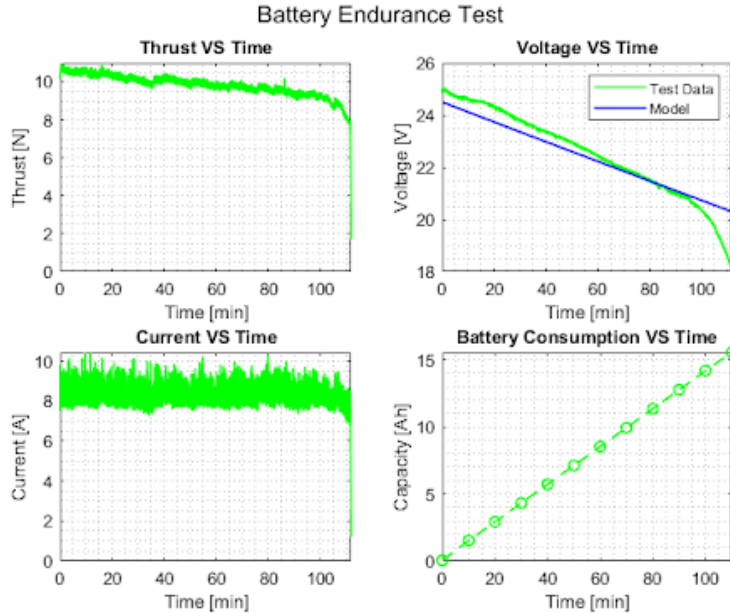


Figure 28: Static Endurance Test Results

With a 16.8Ah, an 8A draw is expected to last around 2.1 hours ideally from full charge (25.2V) to full discharge (15V). Our results showed at around a manually controlled current output of around 8-8.3A, the battery could handle discharge for 1.8 hours before ending the experiment after expected steep voltage drops (note this was not a complete discharge to protect cell health). The voltage curve was also compared to our modeled slope. This test was important in verifying battery pack performance, and functionality after manufacturing. In order to meet a 1 hour flight time, this test was important in proving basic power and propulsion system capability.

5.2.2 Dynamic Endurance Test

The dynamic motor testing is performed in a very similar manner to the static motor testing but can provide more insight to the efficiency of the motors when subjected to cruise conditions. The setup is almost the same, everything is securely mounted onto the dynamic test stand apparatus and now the test stand is then attached to the roof rack of the vehicle and the mounts are securely fastened. During this kind of test, safety was the top priority. So before the test began, it was imperative that we ensured that all aspects of the apparatus were fastened securely and there was no movement from any of the components.

Once the stand is deemed safe and secure, the wiring is connected and ran into the passenger cabin and the preferred testing profile can be loaded into the RC Benchmark UI. The vehicle operator will drive to the desired speed and focus solely on maintaining control of the vehicle. The test rig operator will initiate the test profile when the vehicle has reached appropriate (cruise) testing speeds and ensure data collection is occurring as expected. The motor operator will throttle the motor to different ranges over time. Once the test is complete, the vehicle operator will stop the

vehicle and the test rig will be checked for structural integrity and secure mounting before executing the next test.

Based on aerodynamic data, our propulsion model estimated a cruise flight thrust of about 4N per front motor, as indicated by the target line in Figure 29 and power value of about 77.5W (3A to 4A of current draw). According to our model this will allow a cruise flight time of around 1.5 hours (not including takeoff and landing power draw). The results from this test showed our power draw to be double than expected (150W). Although there is errors and experimental bias, the efficiency of cruise is less than expected. Unfortunately more dynamic tests were not conducted to verify these results further. This will have effect on endurance and needs to be analyzed closer for full mission autonomous flights.

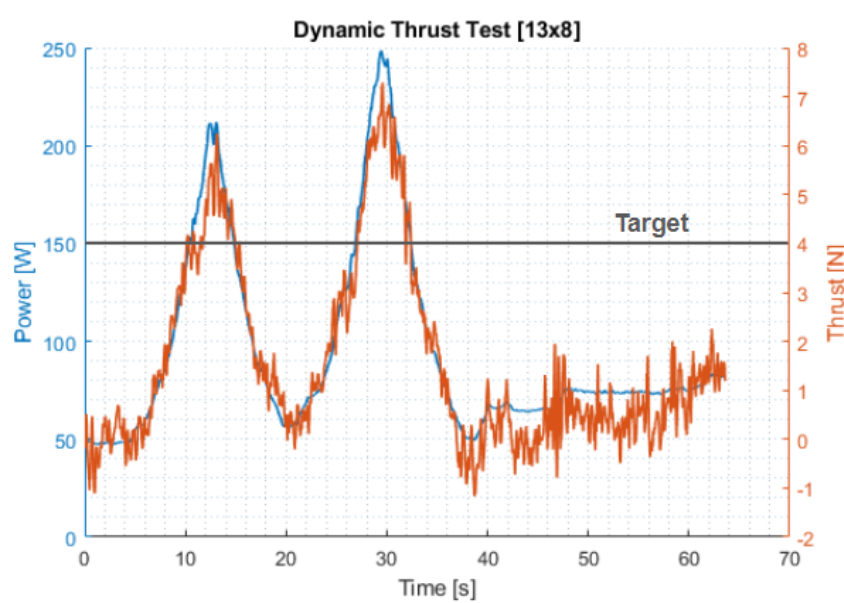


Figure 29: Dynamic Testing Thrust Produced and Power Drawn

5.3 Static Motor Test

In order to verify the requirements for the propulsion subsystem, the manufactured static test stand was used to test the thrust produced and power drawn from the motors in a static environment. To perform the test, the motor, battery, ESC's and propeller were all mounted securely onto the test stand apparatus, wired to the RC Benchmark board and connected to a PC running the RC Benchmark software. Once all pieces are tightened and secure, all team members would stand clear of the plane of rotation while wearing safety glasses. The test was then performed by either manually controlling as needed or executing an automated test profile in the RC Benchmark UI. By utilizing this UI, we were able to measure torque, thrust, voltage, current RPM (optical sensor), power, propeller efficiency and ESC input.

Our propulsion model was based on the test results of German brand aeronaut propellers. Initially, we purchased the aeronaut propellers to verify our models and perform static testing with.

However, due to limited supply and long lead/shipping times for the propellers that we needed, after performing some testing with the aeronauts, cheaper and more readily available APC propellers were bought and tested. The comparison between the two brands of propellers can be seen in the Thrust vs Power plots in Figure 30.

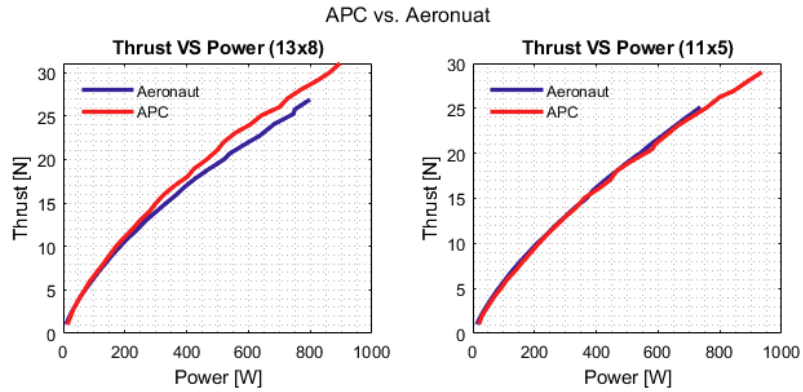


Figure 30: Aeronaut vs APC propellers

Table 5: Brand and Size of Propellers Tested

Propeller Style	Tested Sizes [Diameter x Pitch]		
	Aeronaut Electric Carbon Light	9x5	9x6
10x5		10x6	10x7
11x5		11x7	
12x5		12x7	
13x7		13x8	
APC Thin Electric	11x4.5	11x5.5	
	13x8		

Table 5 shows what sizes, which are given as the propeller diameter by propeller pitch, of propellers along with the corresponding brand that were used during testing. During the initial round of thrust testing, the results showed the rear motor thrust to be insufficient. When a 10 inch propeller was used with a size 2216 motor, to reach the desired thrust we were using the maximum power draw. To correct this, we decided to use both larger propellers and motors which would in turn increase the thrust tolerance for more agile hover and a greater range of aircraft C.G. positions. After various rounds and configurations of tests, we decided on the 13x8 APC electric with the 2820 550KV motor for the front and the 11x5.5 APC electric with the 2820 860KV motor for the rear as they closely lined up with our model.

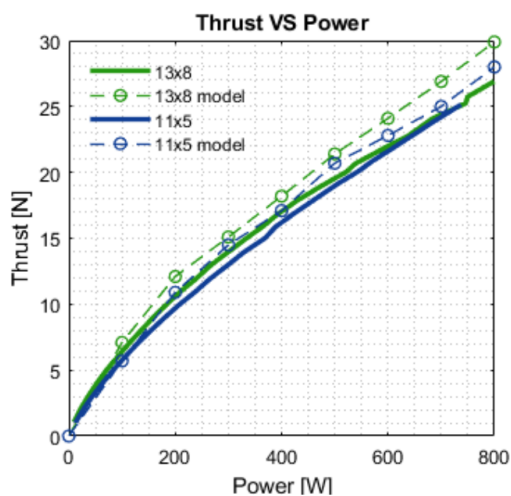


Figure 31: Experimental vs Model Comparison for Static Thrust

5.4 Control Test

The Controls Test involved verifying that all of the control actuators responded correctly to input. Once the servos and ESCs were properly installed in the plane, connected to the PCB, and configured in Mission Planner, testing involved ensuring that they responded as expected both to pilot input and autonomous commands.

Pilot input verification involved ensuring that both ailerons responded to roll input, that the elevator responded to pitch input, and that the tilt servos switched positions when the pilot commanded a switch between fixed-wing and VTOL flight. Pilot input verification also involved ensuring that the actuators responded appropriately to pilot yaw input; This meant that the front ESCs and motors would output differential thrust in fixed-wing flight, and that the tilt servos would deliver vectored yaw in VTOL flight. The final component of pilot input verification involved verifying that the ESCs and motors responded appropriately to throttle input in both VTOL and fixed-wing flight modes.

Autonomous command verification was very similar to pilot input verification. The control surfaces' behavior was verified by changing the attitude of the unarmed aircraft in 'Auto' mode; The correct behavior of the surfaces is to deflect in such a manner as to restore the aircraft to level flight. Autonomous ESC response is verified in a similar manner, but in VTOL flight; The ESCs must command the motors to produce thrust in such a manner as to keep the aircraft level. Finally, the tilt servos' behavior is verified by manually rotating the armed aircraft about its yaw axis and verifying that they respond in such a manner as to oppose this motion.

The controls test was successful, and all control actuators responded correctly to both pilot input and autonomous commands.

5.5 LiDAR Test

Validating the supplementary LiDAR and the according functional and design requirements was done by comparing the recorded measurements of the sensor against the set height of a test rig as

seen on figure 32. The LiDAR was placed on a modified LiDAR bracket and mounted on a test rig purchased online. The test rig was set at different heights and placed over different test "surfaces" water in a bowl, aluminum foil on top of a table, and high grass and branches. These settings were chosen to mimic real surface conditions the system could deal with. The measurements were taken on the LeddarTech Configurator, the off the shelf software package that interfaces with the chosen LeddarOne LiDAR sensor. The results for one test are tabulated below along side the test rig, more tables can be seen in the appendix. The test done over aluminum foil showed that the

Trial #	Set Height(cm)	LiDAR Reading(cm)
1	160.0	166.294 +/- 0.25
2	109.2	114.776 +/- 0.25
3	88.9	94.742 +/- 0.15
4	27.94	33.274 +/- 0.20
5	11	13.732 +/- 0.10

(a) LiDAR Test Data, Over Aluminum Foil



(b) Test Rig, Adjustable Height

Figure 32: LiDAR Test Setup and Results

LiDAR measurements are off by about 7.5 cm, which is below the required 10 cm difference. All the other tests showed better results than this, proving that the LiDAR is hindered by highly reflective surfaces, but not enough for concern. The LiDAR also interfaces with the ground station data logs and shows similar results as with the configurator. Thus design requirement 3.4 is verified, and design requirement 3.5 is closer to being verified as well.

5.6 Car Top Aerodynamic Test

5.6.1 Setup

Once on site, the setup consists of inserting the avionics package into the Drak UAV, making sure the pitot tube is covered while powering on. The battery is plugged in through the power module to the avionics package while laptops are connected to the Arduino Mega board and avionics package to collect data. Mission Planner starts communicating with the avionics package and code is pushed to the Arduino to collect data from the load sensors and accelerometers. Ensure the calibrating process is run on the load sensors to zero out any effects from wind. To calibrate the accelerometers and IMUs, orient the Drak and avionics package in various positions as instructed by the software to ensure that the vehicle pitch and AOA can be properly recognized. Mount the Drak UAV on the test stand at the desired AOA by changing the test stand mount position. Lift and secure the test stand to the vehicle roof using U-bolts. Finally, set up the weather station on the ground by

connecting it to a laptop and taking required static weather condition measurements.

5.6.2 Procedure

First, verify the testing area is clear of any vehicles and people other than the testing vehicles and operators. Next, record the temperature, pressure, wind direction, and wind velocity from the weather station. Start the Arduino and Mission Planner data collection software simultaneously while the vehicle is stationary. Mark down the capture time to the second when the Arduino was started, to assist with data synchronizing later. Accelerate the test vehicle to the desired airspeed velocity, which in this case is 18 m/s, and maintain as constant of a velocity as possible for a minimum of 30 seconds. After at least 30 seconds, end data collection from the Arduino and Mission Planner at the same time and then bring the car to a stop. On the first run of the day, bring up the data from both sources to validate against each other. Finally, download and save the data from the Arduino and Mission Planner. Remove the test stand from the vehicle, adjust the angle of attack as necessary, and repeat the above procedures.

5.6.3 Analysis

The first task of analysis is to extract the aerodynamic forces on the aircraft from the load cell data. Figure 33 gives the free body diagram used to derive equations for these. Equations 1 and 4 give the equations for lift and drag, where θ is the pitch angle of the dynamic test stand itself.

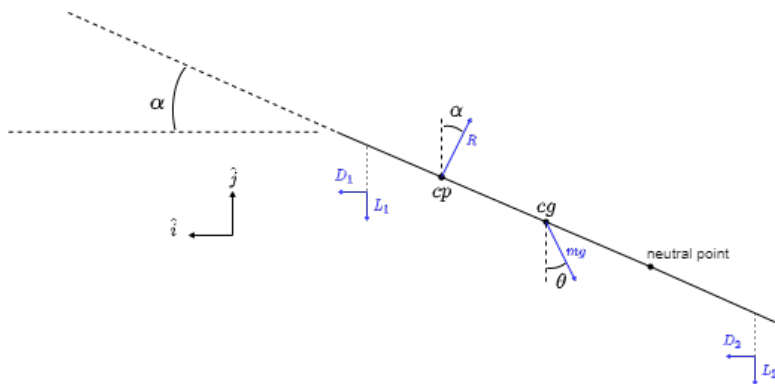


Figure 33: Free Body Diagram of Forces on Aircraft During Dynamic Testing

$$L = R * \cos\alpha \quad (1)$$

$$L = mg * \cos\theta + L_1 + L_2 \quad (2)$$

$$D = R * \sin\alpha \quad (3)$$

$$D = D_1 + D_2 - mg * \sin\theta \quad (4)$$

Once the script has solved for the lift force and drag force, equations 5 and 6 return the aerodynamic coefficients.

$$C_L = \frac{2L}{\rho V^2 A} \quad (5)$$

$$C_D = \frac{2D}{\rho V^2 A} \quad (6)$$

Traditional error propagation methods allow the team to quantify the uncertainty in these aerodynamic coefficients. Since the experiment aims to measure steady-state conditions, batch LLS estimation can be used to quantify the uncertainty on each of the measurements. For unvarying sensor and process noise, this estimation reduces to a statistical average and standard deviation. Next, methods described by Taylor [49] propagate these uncertainties through the preceding equations, to find the uncertainties in these coefficients.

Results

5.7 Hover Testing

Once the individual subsystems were verified, the full system level tests could begin. The first step for hover testing was to verify that the motors could produce more thrust than the weight of the vehicle. This was done by attaching the aircraft to the dynamic test stand and weighing it down with sandbags. Similar to the dynamic testing, the forces applied to the aircraft were observed in relation to the throttle values and confirmed that they were sufficient for vertical takeoff. Initial tests were performed using a safety tether below the aircraft. The results were less than desirable, with the aircraft showing erratic behavior and failing to achieve a stable liftoff. It was thought that the tether below the aircraft could have been causing the controllability issues, and it was replaced with a tether from the ceiling to the aircraft that held it suspended above the ground. This test also resulted in significant rolling behavior when the throttle was increased. These results in combination suggested that the problem did not lie with the tether, so untethered tests were performed. These tests showed the aircraft continuing to roll sharply when the throttle was increased - it was clear that sufficient thrust was being produced to lift the aircraft, but it was not being properly applied to the vehicle. The cause of the controllability problems was now clear: the flight controller. Upon closer inspection of the flight computer configuration parameters, it was discovered that the controller was configured for an aircraft with 4 motors rather than the 3 that are present. Once this was rectified, further hover tests were attempted. The first test after making this change proved the capability of the aircraft to lift itself off the ground. During this test the vehicle achieved a height of approximately 10 cm, and translated a lateral distance of about 3 meters. This was the first successful demonstration of hover capability, and a major milestone for progress of the project.

Further hover tests were performed to improve the responsiveness and behavior of the aircraft, specifically to adjust the PID (Proportional-Integral-Derivative) gains to maintain stability. After several additional short hovers, the gains were established to a reasonable degree, bringing the hover control to near-optimal stability. With hover functionality proven and dialed in, full flight testing is the next step in achieving complete success.

5.8 Flight Testing

Flight testing was the final verification for the project where full system testing could take place. This means ensuring that all the subsystems behave nominally, proper integration of all those subsystems, transition between vertical flight and level flight is successful, the UAS is stable in level flight, and checking the autonomy and endurance requirements. Many flight tests took place so a timeline showing the purpose and results of each test can be seen on figure 34. In terms of functional and design requirements, these tests would be the final verification of all them but more specifically functional requirements 1,2, 3, and 6.

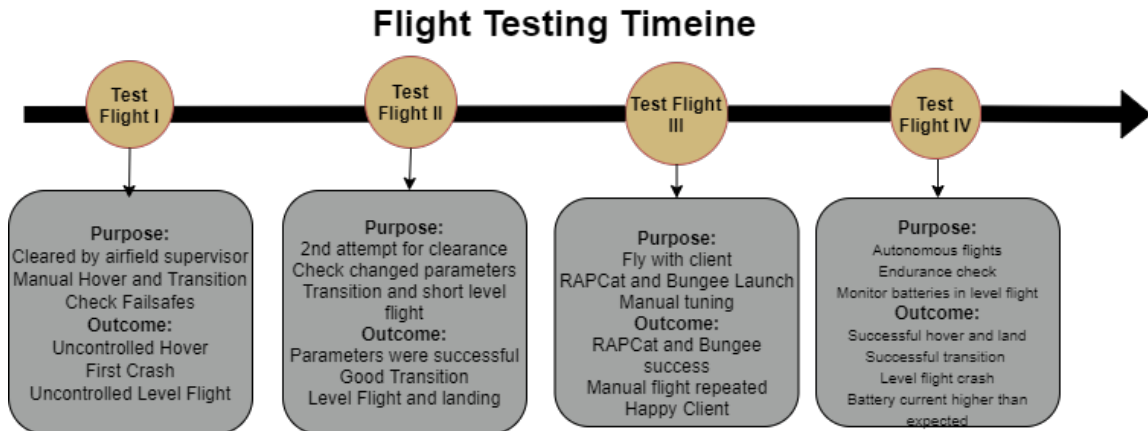


Figure 34: Flight Testing Timeline

Analyzing the test data was done via the data flash logs and telemetry logs saved by the Mission Planner ground station software and visual inspection of videos taken of those tests. What follows is a discussion of each test flight and the major takeaways that lead to the verification of each functional requirement.

The first flight test was the a visceral moment for the group. It ended in tragedy but many lessons were learned which led to the success of the later flight tests. The goal was to perform a basic hover and landing to further calibrate any last minute parameters and a transition to level flight mode as was done two days prior. This would all be done in front of the airfield supervisor who grant us clearance to use the airfield upon completion of these demonstrations. However, due to the rushed nature of the day, many pre-flight checks were not completed and a simple hover test turned into an uncontrollable glide leading to a crash. The flight path taken by the UAS can be seen in figure 35; which was rendered using google maps.

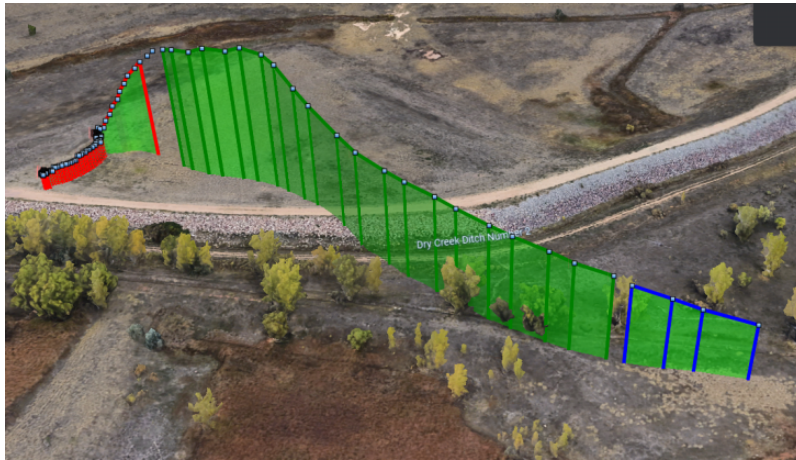


Figure 35: Google Maps Render of First Flight Test Flight Path

The pre-flight checks are done to make sure that the compass, gps, and most importantly our kalman filters, the algorithms used by the flight controller to estimate the location and attitude of the plane, are behaving correctly. In addition, the team added multiple fail safe protocols in the case of a loss in RC connection, along with a geofence. This process was unfortunately rushed the day of the first test and all the required aspects were not properly checked. This resulted in the kalman filters diverging from the start and inaccurate airspeed measurements.

The hover portion of the flight is where the majority of the issues occurred. The winds at 100 feet in the air were strong and the craft was behaving erratically and the pilot in an attempt to salvage the flight, transitioned between hover and level flight mode much too quickly. There are set conditions that are required to fully transition into the level flight mode, and the flight controller ignores pilot input while trying to do so. The pilot tried to cut the throttle to land it after noticing the sudden rise in altitude, but because of the quick transitions the flight controller kept thrusting and the plane flew even higher. This can be seen in the hover thrust curves from the data logs.³⁶



Figure 36: Hover Thrust Logs from Flight Test 1

The red line depicts the commanded thrust monitored by the groundstation software. Note the beginning of the curve; the pilot clearly had control at the beginning as can be seen by the rapid small spikes. Then note the multiple mode switches in the message blocks below which show the rapid transitions between flight modes. The thrust curve hits zero, showing the pilot tried to cut the throttle, but it jumped back up because the flight controller took control in an attempt to fulfill the transition requirements. This led to the UAS gaining in altitude and the pilot not having control.

This then leads to the transition and level flight phase. Again, due to rapid transition between modes, the flight controller ignored pilot input and tried to reach the forward motors condition that is required for level flight. The servo tilt rates were set way too low, 15deg/sec, which would take a grueling 6 seconds to reach horizontal forward motor position, so the transition phase was prolonged and eventually led to wing stall. The plane did a barrel roll and then leveled out to glide over the trees until it crashed.

While gliding, the pilot was unable to control the UAS and this was because of the kalman filters. Figure 37 shows the desired and actual roll values measured by the flight controller kalman filters. There was a clear -15 degree bias in the roll at the beginning, so while in level flight mode, the pilot was trying to roll left but the aircraft only sensed a 5 degree bank instead of the full roll left command. This is clear by the slight curve in the flight path 35 and can be seen in data logs. The pilot was unable to bank out of the glide.



Figure 37: Desired and Actual Roll Plots from Flight Test 1

After this first crash, the group had a couple of really important takeaways. Mainly re-configuring the sensor parameters. For example the pitot tube was configured as an analog sensor on the ground station, but its actually a digital sensor with an I2C protocol. A lot of airspeed issues occurred because of that. The servo tilt rate parameter was way too low, so that was increased to a 60deg/sec. Ultimately this test led to a much more robust pre-flight check procedure which allowed us to perform better in later flight tests.

The second flight test went much better as a result of the lessons learned in the first crash. The goals of the second flight test was to try and get clearance from the airfield supervisor by demonstrating a hover and transition Changing the servo-tilt rates to 60deg/sec, changing the pitot tube measurements to digital, and re-calibrating all the IMUs for better kalman filter accuracy made the difference and the test ended in success. Before the test the group further tuned the

hover PID gains to eliminate the yaw oscillations that were persistent during the first test and this resulted in a successful hover to 10 meters with no erratic behavior due to wind.

A complete transition to level flight mode was executed and a stable manual level flight was completed as well. During the level flight phase, the UAS was observed to be stable and responding to all pilot commands. Finally, a complete transition back to hover mode was executed and the aircraft was landed with no damage. Overall, this test was a success. However, there were some issues with pitch stability during level flight mode and the compass not behaving nominally.

Strong gusts of wind were causing the plane to pitch forward abruptly. This was controllable however and did not result in any crashes. Secondly, the compass was found to be behaving poorly and giving in-correct heading readings, which made it difficult for the UAS to weather vane into the wind. This led to unstable behavior in yaw and pitch attitudes. Regardless, the team was elated by the success and was ready to move on to level flight tuning and executing autonomous missions. Functional requirement 1 was verified in this test, along with functional requirement 5.

The third flight test was a day to show the client the team's progress. Functional Requirement 6 was the primary verification to be complete that day. The UAS integrated with the RAPCat system via the 3D printed RAPCat hook fastened to the bottom of the fuselage. Once launched, it was manually piloted and flew in level flight mode until returning to VTOL mode and landing. Figure 38 shows the flight path taken that day after the successful RAPCat launch.

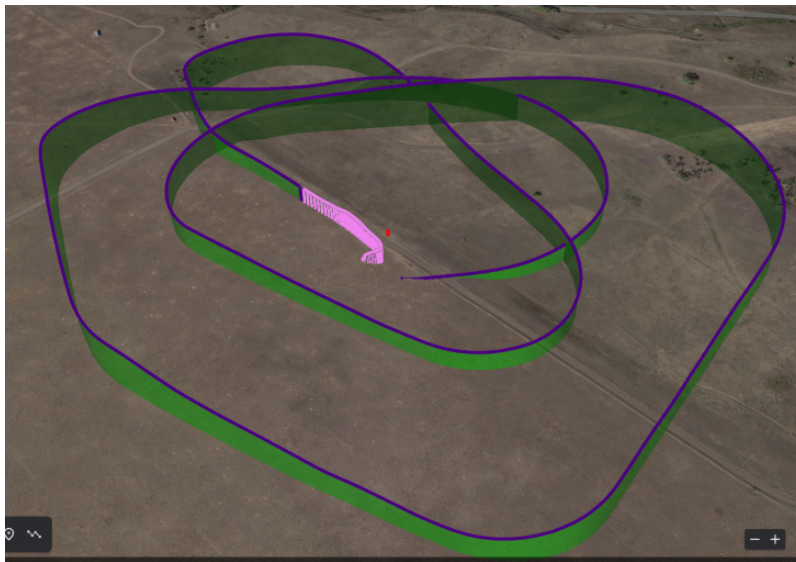


Figure 38: Flight Path, Third Flight Test

The UAS performed well and showed that it was capable of withstanding the 4.24g load from the RAPCat launch, so functional requirement 6 was verified. This third test day meant that the team could move forward with attempting autonomous missions and moving closer to verifying the final functional requirements. Figure 39 shows the UAS launching off of the RAPCat system. Further discussion on RAPCat integration and the test is found in next section.



Figure 39: RAPCat Launch, Third Flight Test

The most recent test was meant to verify the last of the functional requirements but most importantly functional requirements 2 and 3 by conducting multiple short autonomous mission followed by one long endurance mission. The missions were created on the Mission planner ground station software and were as follows: first a short hover and quick landing, then another hover to above 15m high, then a mission with a transition to level flight mode for a short loiter, followed by final long endurance level flight mission.

The UAS executed both the short and elevated hover missions without any issues. Figure 40 shows the altitude throughout the low hover mission, along with messages showing that it was progressing through the autonomous mission properly. It behaved nominally and was capable of landing at a slow rate to mitigate the risks of prop wash, which causes the propellers to stall. The descent was a chosen parameter. The PID gains chosen after the rigorous hover testing really showed in these early autonomous missions. The flight controller was able to stabilize the UAS in hover mode without any issues. The UAS also executed the transition in level flight perfectly as well. However, during the level flight phase of this test, the UAS started to lose altitude and suddenly crashed.

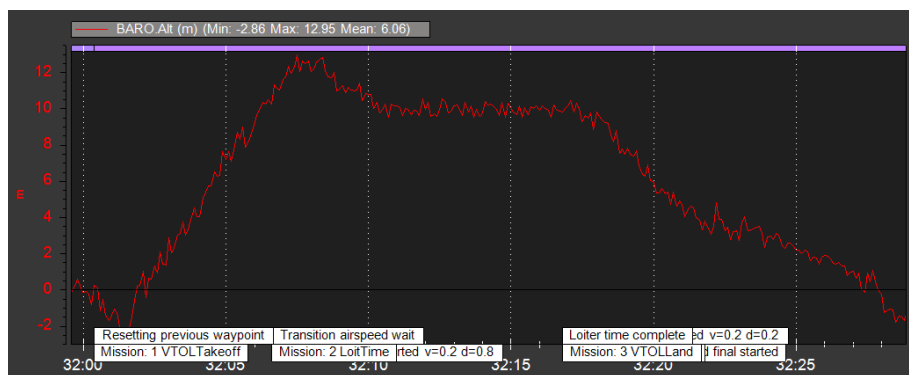


Figure 40: Altitude During Autonomous Hover Mission

Shortly after the transition, the UAS started losing altitude at a steady rate. Although the UAS was following a pre-planned mission, the pilot can flip back to manual code to recover it in the case of a crash. The pilot did so and throttled up and banked to recover from the fall. It started to re-gain its altitude but was being unresponsive to all pilot inputs and crashed into the ground at 80 mph shortly after. While this was initially disheartening, the progress made that day made up for the crash and the analysis afterward cleared up a lot of previous questions.

After reviewing the data logs from the test, it was clear that the kalman filters again influenced to start estimate the wrong altitude data which led to the UAS being unresponsive. This time however it was heavily affecting the pitch estimation which led to the sudden crash. A kalman filter uses an algorithm that attributes weights to the system dynamics and sensor data to estimate the state. False sensor readings are typically the main cause of wrong filter data. There was a thorough calibration done on the plane done the day before so the IMU's, pitot tube, or the gps could not have been the issue. After speaking to the client and looking up this issue on the ArduPilot forums, the team looked at the compass data in the data logs.

The compass is a part of the gps and informs the control algorithms with heading and attitude measurements. by measuring external magnetic fields. It was observed in the data logs that right before the crash the compass gave an erroneous pitch reading which would have caused the EKF to have a pitch bias. The client advised that the compass could be affected by any magnetic fields that the avionics package could be creating. Namely the ESC's as they require a large current draw at a very fast rate, sometimes 100 Amps in a very short amount of time. The team believes that due to the pilot trying to command a throttle up when the UAS was losing altitude, the ESC's created a large magnetic field that swayed the compass readings and led to a sudden crash. This can be seen in figure 41

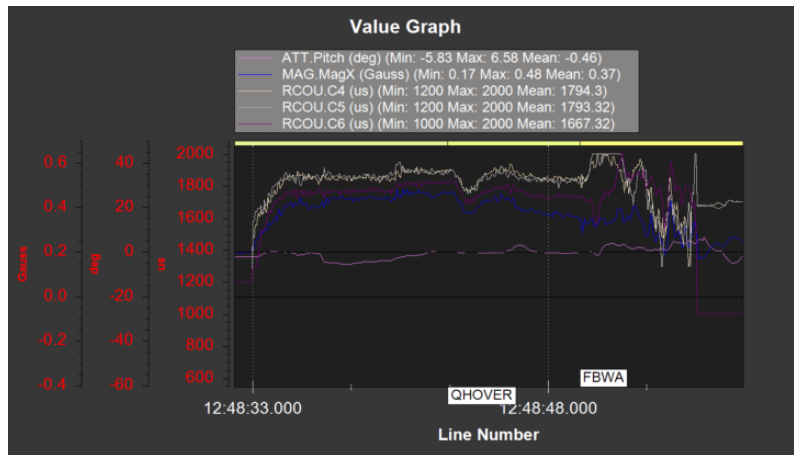


Figure 41: RAPCat Launch, Third Flight Test

The legend above the figure shows what is being plotted, RCOU4, RCOU5, and RCOU6, are the ESCs commanded PWM values while MAG is the compass reading. It can be seen that the compass moves rapidly to a negative pitch reading before the crash right when the ESC's were commanded to throttle up. While these are not conclusive results, this shows that the compass could have been effected by an induced magnetic field from the ESC's current draw.

#	Category	Description	Consequence	Probability	Impact	Risk Level	Risk Modification Plan	Residual Risk
5	Supply/Struct	Drak kit backordered, potential supply difficulties	Would not be able to produce second deliverable for customer, may not have backup parts in case of destruction	High	Medium	High	Utilize IRISS' existing connection with RiteWing to obtain wing kits outside of standard commercial production	Medium
8	Propulsion	Battery damage during pack assembly	Fire/explosion in battery cells, injury to personnel	Low	High	High	Ensure spot welder is only used by properly trained individuals, follow strict safety protocols when working with battery cells	Medium
11	Testing	Car-top safety considerations	Damage to vehicles, test equipment, citations issued for property damage or other unknown reasons (?)	Low	High	High	Coordinate with department to create safe testing procedures and equipment, research local laws to ensure legality of test operations	Medium
12	Structures	Inaccurate FEM model	Possible material failure, could need to redesign parts	Medium	Medium	Medium	Compare FEM to known models and research minimizing FEM error, continually refine models	Low

Figure 42: Primary Risks of VORTEX Project

Moving forward, the team would like to have the gps be re-located to the horizontal stabilizer. The avionics package and ESC's interfere with the compass too much for any future autonomous missions to be successful. The team is planning another flight and is exploring options to mitigate any other magnetic interference such as parameters from the ArduPilot documentation and further tuning.

6 Risk Assessment and Mitigation

Early in the project, it was critical to evaluate the risks that may be involved through the lifespan of the project. In the interest of brevity, only the highest risks are shown in the table below. These risks were developed through experience with RC aircraft and consultation with faculty and the customer. These risks were tracked using a simple chart, and the mitigation strategies were applied from the start where applicable.

The biggest risks for the project were primarily with safety considerations. The custom battery packs have risk of fire or explosion if they are not handled correctly during fabrication, and the dynamic tests have risk of injury to people or property. In order to mitigate these risks, safety procedures were developed and verified by the PAB before any fabrication or tests were performed. During the course of the year, the only significant risks that ended up being present were in the aforementioned fabrication of the batteries and the dynamic tests. The mitigation plans can be considered successful, as the severe outcomes of the risks were avoided and the ones that were encountered, such as shipping delays, were not a major hindrance to the progress of the project.

7 Project Planning

Section Authors: Bill Chabot, Justin Troche

The VORTEX Team is broken into sub-teams, determined predominantly by the subsystems of the aircraft and its functions. The team operates mostly through collaborative effort and decision making, rather than a top-down hierarchy. When necessary, the Project Manager can make a final decision if there is not consensus among the team members relevant to the decision at hand. These roles and relationships can be seen in the Organizational Chart below.

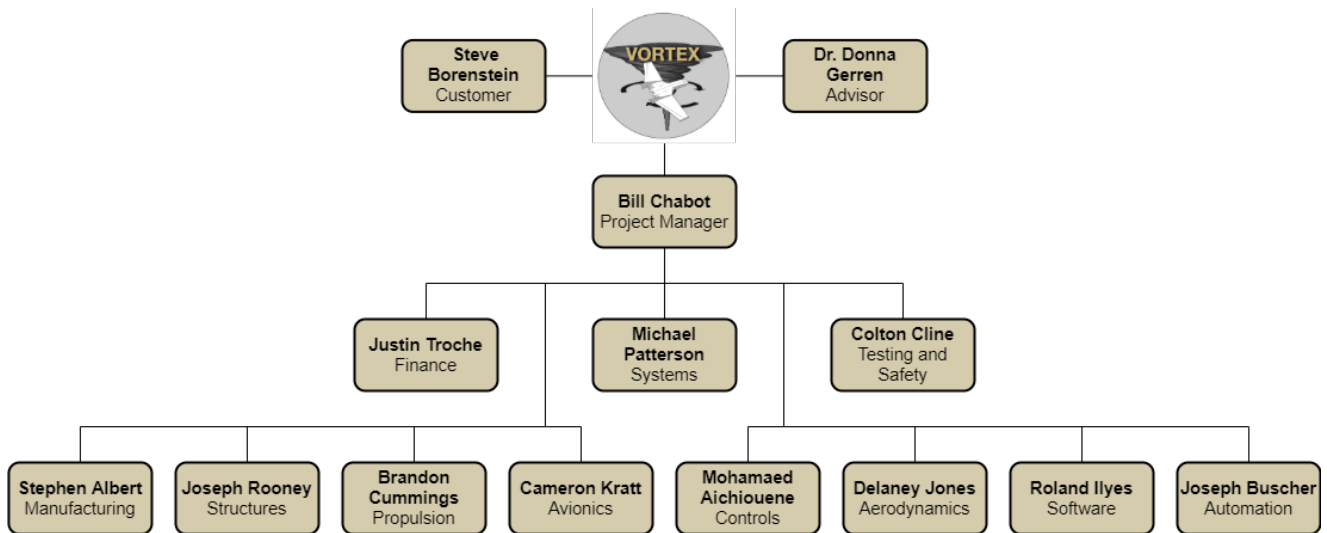


Figure 43: Org Chart

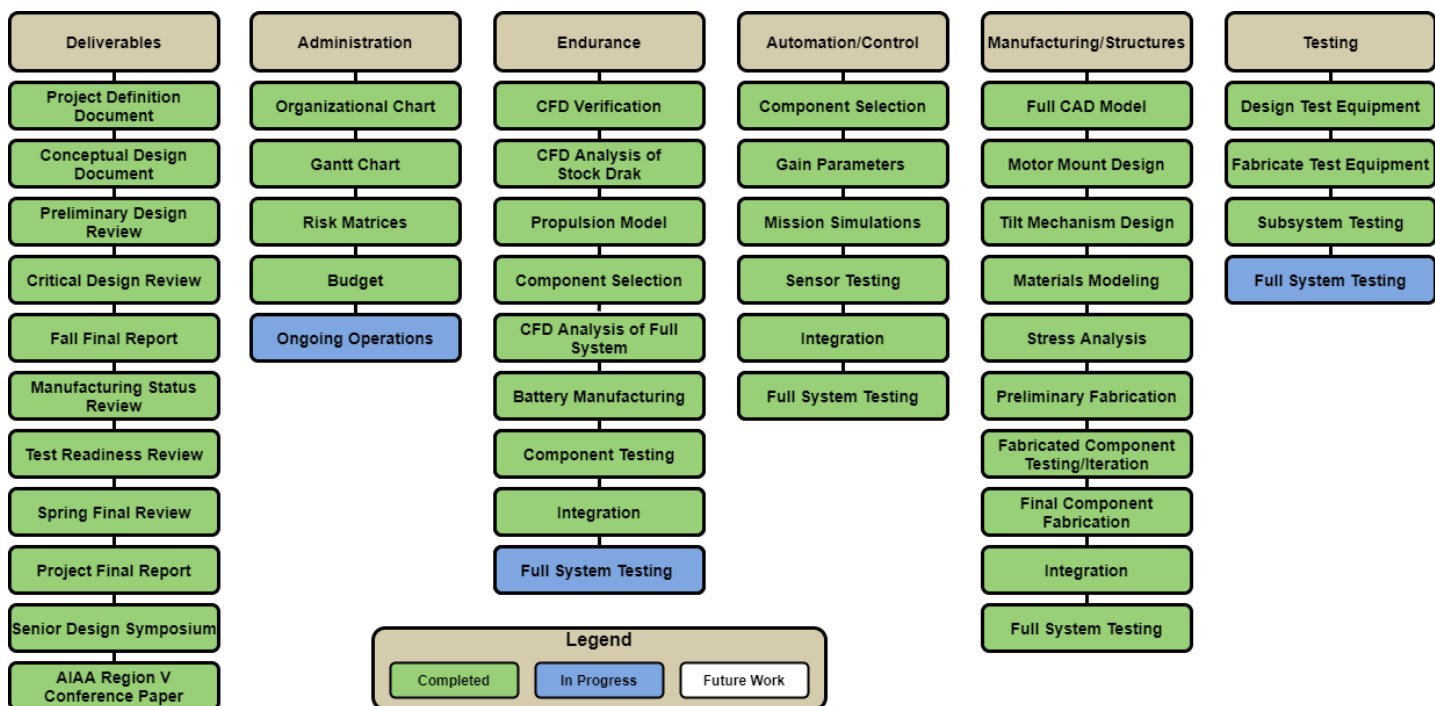


Figure 44: WBS

The Work Breakdown Structure shown above outlines the general flow of tasks to be done by each subteam. The first semester of the project saw the design phase and beginning of fabrication be completed. The second semester was where the majority of the engineering process was executed, with fabrication and testing being the primary focus. These were determined by looking at the individual subsystems of the aircraft and the associated tasks to achieve success for each subsystem. With all subteams assigned and a plan laid out, a clear path to success was established. The tasks from the WBS were then further detailed and laid out chronologically in the form of a Gantt chart.

Margins were determined based on the complexity of the task, with simple tasks and tests being given margins of 1 or 2 days, with complex undertakings such as aerodynamic FEM refinements being given a week or more of margin. Similar to the WBS, the general flow of tasks consisted of: finishing models, initial fabrication and testing, followed by final fabrication, assembly, and flight testing. The critical path was determined by finding the key tasks without which the project could not be completed successfully. They consist of the following: Fabricating all necessary test equipment, battery fabrication and testing, material and component failure testing, avionics package integration, final fabrication and flight testing. The modeling and refinement for specific components could only continue for so long before it began impeding the progress of actual fabrication and the payoff was no longer worth the time invested. Failure testing cheap 3D printed PETG parts will be much more valuable to obtaining useable data that will help determine the final component design than it would be to continue spending time refining a CAD force model that is inaccurate but is trustworthy enough to be on the right order of magnitude and not cause wildly unexpected results.

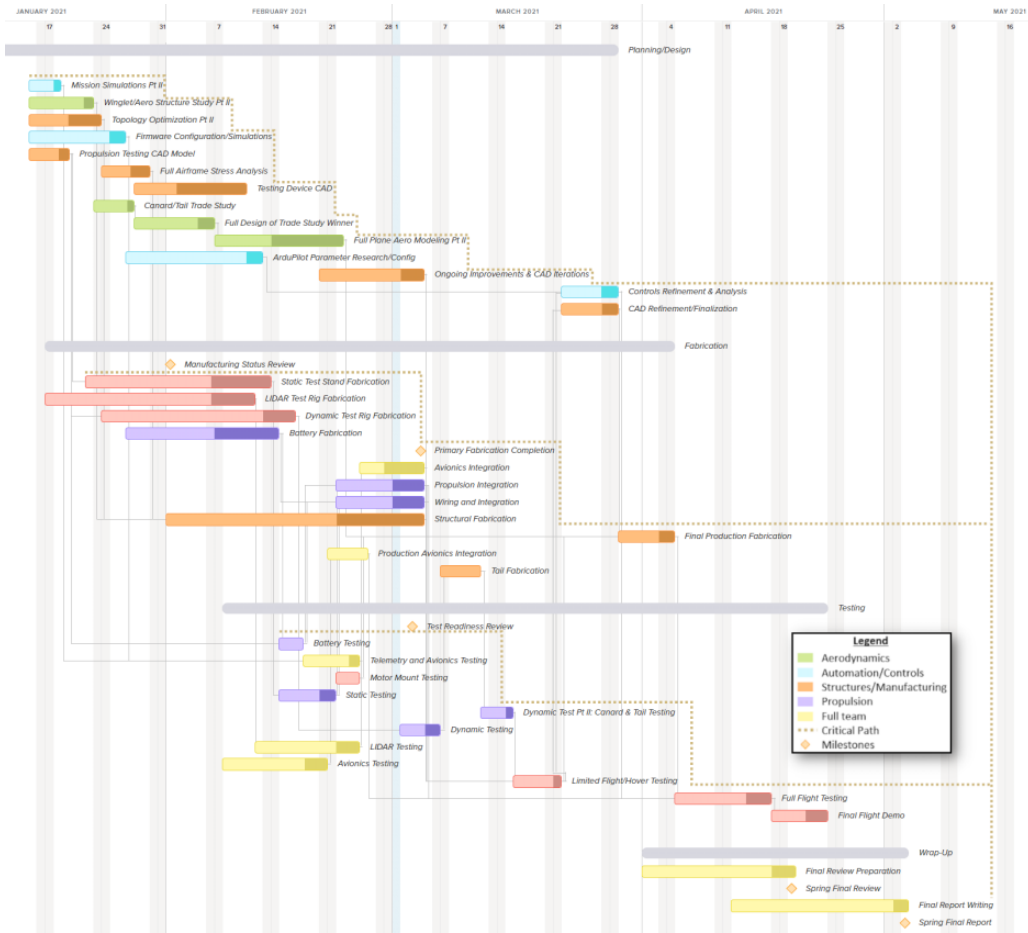
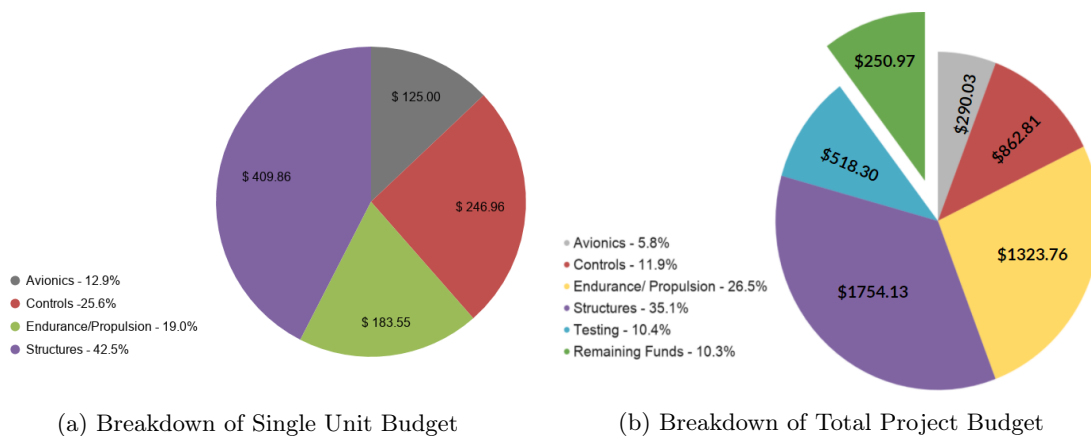


Figure 45: Gantt Chart



The two pie charts above give a brief overview of the budget breakdown for both the single unit and total project budgets, broken down by subsystems, showing the corresponding values and percentages for each. As per functional requirement 7, the budget for a single unit must be no more than \$1000, not including any batteries or avionics. The actual cost for a single unit based on the parts shown in the full budget table is \$965.37, which puts us \$34.63 under the single unit budget with a margin of 3.46%. With a total project budget of \$5000, this enabled us to allot enough money to manufacture two full units, have a budget of \$500 for testing and a 20% budget for any contingencies or complications. Taking that initial budget allotment and comparing it to the actual budget as shown in 46b, it shows that the team stayed within this loose guideline. The actual testing budget went slightly over, but since the entire contingency budget did not need to be used this allowed for a bit more freedom throughout all of the subsystems.

As far as individual subsystem margins, the smallest margins were in Avionics (the only Avionics part that is included in the unit budget is the LIDAR sensor) and Structures. Structures has the smallest due to the requirement of using the Drak kit and its fixed price. Similarly, Avionics has just the LIDAR sensor that has a small margin if we wanted to purchase a slightly more expensive sensor. For the overall budget, the margin for Controls ended up being the only negative margin due to some unforeseen issues with servos. Some of the cheaper servos were not able to withstand the loads that were placed on them during flight. In addition, more servos needed to be purchased after a crash during testing. However, other subsystems were well under budget allowing for this to happen without issue. Even after these issues and with this negative margin, we finished the project with a remaining balance of \$250.97.

8 Lessons Learned

1. Organization is key from day one, both physically and digitally
2. Scope the project to what is achievable within two semesters - your customer will be happier with a slightly less ambitious project that you can deliver on rather than a half-finished project that's out of the realm of possibility
3. You are allowed to give pushback to the PAB - stand up for your decisions and back them up with valid data and justification

4. Maintain clear communication between all team members and check it frequently
5. Write clear requirements breakdown
6. Write cross system requirements
7. Write **and use** clear pre-flight checklists
8. Arm the GPS
9. Turn it off and back on again
10. Set toaster BELOW 350F before putting the PCB inside

9 Individual Report Contributions

Table 6: Report Contributions

Team Member	PFR Contribution
Mohamed Aichiouene	Control Modeling and Mechanisms, Avionics Implementation and Testing, Empennage Design, and General Testing
Stephen Albert	Title page, Manufacturing, Assembly and Integration, Stock Drak Body, Forgot to arm the GPS
Joseph Buescher	Project Objectives, Automated Flight Design, Empennage; & Test Stand Manufacturing
Bill Chabot	Introduction/Information, Project Purpose, Final Design, Manufacturing, & Project Planning, Pilot, PCB Baker
Colton Cline	Manufacturing: Test Stands; Verification and Validation: Wing Motor Arm Stress Testing, Car Top Aerodynamic Test
Brandon Cummings	Propulsion final design, Battery Manufacturing, Endurance verification
Roland Ilyes	Controls Verification, Firmware Final Design, and Flight Testing, Broke a servo, Forgot to arm the GPS
Delaney Jones	Aerodynamics
Cameron Kratt	Project purpose, avionics FBD with explanation, avionics final design
Michael Patterson	Armed the GPS, FBD, Editing, Final Design, Project Objective and Functional Requirements
Joseph Rooney	3.3: structures, 4.1: motor mounts, 5.1: Stress Test
Justin Troche	Title Page, CONOPs, Verification and Validation: Dynamic Endurance Test, Static Motor Test, Project Planning: Budget, Editing/Proofreading/Formatting

References

- [1] Borenstein, Steve. "IRISS VTOL" Presentation, University of Colorado Boulder
- [2] Integrated Remote and In-Situ Sensing. Retrieved September 14, 2020 from <https://www.colorado.edu/iriss/content/our-capabilities>
- [3] Glezellis, John. "Control Surface Deflection Accuracy." Model Airplane News, 16 July 2015, www.modelairplanenews.com/control-surface-deflection-accuracy/.
- [4] Admin. "Advantages and Disadvantages of RADAR Systems." LiDAR and RADAR Information, 21 Nov. 2017, LiDARradar.com/info/advantages-and-disadvantages-of-radar-systems
- [5] Etkins, Bernard, and Lloyd Duff Reid. Aircraft Dynamics, Stability and Control. 3rd ed., John Wiley & Sons Inc., 1996.
- [6] Alex. "Complete List of Flight Controller Firmware..." DroneTrest Blog, DroneTrest, 9 June 2018, blog.dronetrest.com/flight-controller-firmware/
- [7] Chen, Zaibin, and Hongguang Jia. "Design of Flight Control System for a Novel Tilt-Rotor UAV." Complexity, Hindawi, 13 Mar. 2020, www.hindawi.com/journals/complexity/2020/4757381/
- [8] "Drones With Long Flight Times: Fixed-Wing VTOL: Commercial Drones |." HSE, 18 Sept. 2020, hse-uav.com/product/sp9-vtol-drone/
- [9] Ivankov, Alex. "Advantages and Disadvantages of LiDAR." Profolus, 22 Apr. 2020, www.profolus.com/topics/advantages-and-disadvantages-of-LiDAR/
- [10] Jackson, Jelliffe. "Project Definition Document (PDD)", University of Colorado-Boulder, Retrieved August 31, 2020 from <https://canvas.colorado.edu>
- [11] "JUMP 20 VTOL Unmanned Aerial Vehicle." Naval Technology@2x, 25 Sept. 2020, www.naval-technology.com/projects/jump-20-vtol-unmanned-aerial-vehicle/
- [12] Labine, Dakota. "Project Definition Document - EMU", University of Colorado-Boulder, Retrieved September 2, 2020 from <https://www.colorado.edu/aerospace/current-students/undergraduates/senior-design-projects/past-senior-projects/2019-2020/endurance>
- [13] "LIDAR-Lite v3." SEN-14032 - SparkFun Electronics, www.sparkfun.com/products/14032.
- [14] "SF11/B (50 m)." LightWare, LightWare LiDAR, lightwarelidar.com/collections/frontpage/products/sf11-b-50-m.
- [15] "PixhawkFamily." PixhawkFamily - LambDrive.com, LambDrive, Ltd, 13 Apr. 2016, www.lambdrive.com/depot/Robotics/Controller/PixhawkFamily/.
- [16] Ebeid, Emad Samuel Malki & Skriver, Martin & Terkildsen, Kristian Jensen, Kjeld & Schultz, Ulrik. (2018). A Survey of Open-Source UAV Flight Controllers and Flight Simulators. Microprocessors and Microsystems. 61. 10.1016/j.micpro.2018.05.002.

- [17] Perroud, David. "VTOL Drone for Mapping and Surveying – WingtraOne." Wingtra, Wingtra, 24 July 2020, wingtra.com/why-wingtra/vtol-drone/
- [18] Range and Endurance Estimates for Battery-Powered Aircraft. www.researchgate.net/publication/269567470RangeandEnduranceEstimatesforBattery-PoweredAircraft
- [19] "RCWL 0516 Microwave Micro Wave Radar Sensor Switch Board Human Body Induction Sensor Module" AliExpress, www.aliexpress.com/i/33011567518.html.
- [20] RiteWing RC - Drak Wing Set Manufacturer <https://RiteWingrc.com/product/RiteWing-Drak-kit/>
- [21] "Tactic Air Drone." This 99 Drone Is 2019's Hottest Gift, today.topdeals.guide/tactic-air-drone-review.5bddafd7a619fd66?v1=drone
- [22] Technologies, Vertical. "Home." DeltaQuad VTOL UAV, www.deltaquad.com/
- [23] "UAVs for Professionals." Innovative Unmanned Systems - FLYTECH UAV, www.flytechuav.com/uav-birdie.html
- [24] "Ultrasonic Sensors: Answers to Frequently Asked Questions." Banner Engineering, www.bannerengineering.com/us/en/company/expert-insights/ultrasonic-sensors-101.html
- [25] "Ultrasonic Sonar Sensor HC-SR04." Génération Robots, www.generationrobots.com/en/401575-hc-sr04-sonar-sensor.html.
- [26] "Vector - The 2in1 Vertical Take-off Tactical UAV - Quantum-Systems." Quantum, 13 July 2020, www.quantum-systems.com/project/vector/
- [27] Vog1 1 - Passively Coupled VTOL Tiltrotor, vogi-vtol.com/
- [28] "VTOL UAV." Airborne Drones, 22 Sept. 2020, www.airbornedrones.co/vtol-uav/
- [29] "VTOL Unmanned Aircraft System – US-Built UAS for Energy and Utility Inspection." ULC Robotics, ulcrobotics.com/network-innovation-and-energy-industry-research-and-development/vtol-fixed-wing-uas/
- [30] Workshop, Dronebot. "LASER vs Ultrasonic - Distance Sensor Tests." DroneBot Workshop, Publisher Name Dronebot Workshop Publisher Logo, 29 Dec. 2019, dronebotworkshop.com/laser-vs-ultrasonic-distance-sensor-tests/
- [31] Ximin Lyu, Haowei Gu. "Simulation and Flight Experiments of a Quadrotor Tail Sitter." SAGE Journals, journals.sagepub.com/doi/full/10.1177/1756829318813633
- [32] "What's the Best Battery?" Advantages and Limitations of the Different Types of Batteries - Battery University, batteryuniversity.com/learn/archive/whats_the_best_battery
- [33] "Types of Lithium Ion." Battery University, https://batteryuniversity.com/learn/article/types_of_lithium_ion
- [34] "LiPo Batteries: A Drone User's Guide." dronegenuity, <https://www.dronegenuity.com/lipo-drone-batteries-users-guide/#:~:text=Lithium>

- [35] "RC Battery Guide: The Basics of Lithium-Polymer Batteries." tested, <https://www.tested.com/tech/502351-rc-battery-guide-basics-lithium-polymer-batteries/>
- [36] "Lithium Iron Phosphate vs. Lithium Ion differences and advantages." epectec, <https://blog.epectec.com/lithium-iron-phosphate-vs-lithium-ion-differences-and-advantages>
- [37] "A rotor- Tilt-free tricopter UAV: Design, modelling, and stability control. International Journal of Mechatronics and Automation. Sababha, Belal & Alzubi, Hamzeh & Rawashdeh, Osamah. (2015) https://www.researchgate.net/publication/301379428_A_rotor-_Tilt-free_tricopter_UAV_Design_modelling_and_stability_control"
- [38] Hrishikeshavan, Vikram and Chopra, Inderjit. "Design and Testing of a Dual Tilt-Wing Micro Air Vehicle". Alfred Gessow Rotorcraft Center, Department of Aerospace Engineering, University of Maryland. https://www.researchgate.net/publication/280841396_Design_and_Testing_of_a_Dual_Tilt-Wing_Micro_Air_Vehicle
- [39] Quadcopter 101, director. XK X450 Aviator VTOL RC Airplane Flight Test Review. Youtube.com, 23 Sept. 2019, www.youtube.com/watch?v=fv0zRxM9V3k.
- [40] Quantum Systems GmbH, director. Quantum-Systems™ VTOL Transition Fixed Wing UAV. Youtube.com, 9 Oct. 2014, www.youtube.com/watch?v=gIheugU1qY8.
- [41] Apkarian, Jacob. "Pitch-Decoupled Tilt-Motor Aircraft with Continuously Variable Transition." Coriolis G Corporation, 2017.
- [42] "ATMOS UAV: VTOL Drones for Mapping & Surveying." ATMOS UAV | VTOL Drones for Mapping & Surveying, www.atmosuav.com/.
- [43] "V-BAT - Industry Leading VTOL: Unmanned Aerial System." Martin UAV, 14 Sept. 2020, martinuav.com/.
- [44] Technologies, Vertical. "The DeltaQuad." DeltaQuad VTOL UAV, www.deltaquad.com/.
- [45] NASA. "VTOL UAV With the Cruise Efficiency of a Conventional Fixed Wing UAV." NASA, NASA, technology.nasa.gov/patent/LAR-TOPS-241.
- [46] "Low Reynolds Number Vehicles", by Thomas J. Mueller, AGARD, 1985
- [47] "APM Powered Tiltrotor." Mike Remaly, Trevor Strand, 2014, https://wiki.dronecode.org/_media/u07.ardupilot_vtol_-_trevor_strand_and_mike_remaly.pdf. Powerpoint Presentation.
- [48] Mooch, "List of Battery Tests" Available: <https://www.e-cigarette-forum.com/blog-entry/list-of-battery-tests.7436/>
- [49] Taylor, John R. "An Introduction to Error Analysis: The Study of Uncertainties in Physical Measurements", 1996, 2nd edition, University Science Books
- [50] Tulapurkara, E. G. "Lecture 17 Directional Static Stability and Control - 2", lecture notes, Dept of Aerospace Engg., IIT Madras.

Appendix A: Additional Trade Study Information

9.1 Sensor Conceptual Design

Criteria	Weight (%)	Rationale
Complexity	25	The ease of interfacing the landing sensor with the existing avionics package is very important, as a sensor that requires extra hardware and software development adds extra work and weight.
Accuracy and Consistency	25	The sensor must be capable of capturing data with enough accuracy to ensure safe autopilot controlled takeoff and landing. The sensor must be able to consistently capture altimeter data in non-ideal conditions (e.g. wind and dust debris).
Size and Weight	20	The heavier and larger the sensor package is, the more of a negative affect it has on the center of gravity location and more additional space it requires.
Cost	15	The sensor package must not be so expensive as to push the project over budget and therefore restrict other design choices on a cost basis.
Resilience	15	It is critical to have sensors that are capable of bearing the forces exerted on it during all testing and mission flights. Constant recalibration and/or replacement needs to be avoided.
Total	100	

Table 7: Landing Sensor Trade Study Weighting

9.1.1 Scale Assignment

Landing Sensors Criteria Standards					
Criteria	1	2	3	4	5
Complexity	N/A	N/A	Requires an external processor for computations and sensor interfacing. Requires external hardware for mounting.	Requires external processor and sensor mounting to interface with avionics system. Does not require external hardware for mounting.	Interfaces directly with the avionics system and uses the internal avionics package MCU to handle all necessary computations.
Accuracy and Consistency	Sensor accuracy greatly effected by adverse weather conditions.	N/A	Sensor fairly accurate in most weather conditions.	N/A	Sensor very accurate in all weather conditions.
Size and Weight	Sensor package significantly impacts CG location and thrust required.	N/A	Sensor package moderately impacts CG location and thrust required.	N/A	Sensor package minimally impacts CG location and thrust required.
Resiliency	Delicate sensor package, requires extra consideration for safe mounting. Requires frequent recalibration.	N/A	A more rugged sensor package. Better handles flight loads and debris. Requires occasional recalibration.	N/A	Sensor package unaffected by flight loads and debris. Recalibration seldom required.
Cost	Sensor package results in high cost to budget.	N/A	Sensor package results in moderate cost to budget.	N/A	Sensor package results in low cost to budget. <100

Table 8: Scale Assessment of Landing Sensors

9.2 Firmware Conceptual Design

9.2.1 Flight Controller Firmware Criteria Standards

Criteria	Weight (%)	Rationale
Functionality	30	The flight controller firmware package must be designed to fulfill the full range of requirements for mission success. Integration with the firmware package, having a capable and approachable GSC, and capability to control VTOL configurations are the the most critical element when choosing an appropriate firmware package.
Resources	30	Access to online resources that detail the use and capabilities of each firmware package is critical to successfully executing a mission. A firmware that has an extensive site for forums, tutorials, and open information, especially on VTOL flight configurations, will be very helpful.
Customer Preference	25	This final project is meant to integrate into the customer's existing aircraft systems, so the firmware choice should fall in line with the customer's preference to minimize difficulty of integration.
Hardware/Software Interface	15	A flight controller firmware that is easily integrated with the chosen avionics package, ground station software, and flight planner is critical to minimize weight and number of electronic connections and mechanisms.
Total	100	

Table 9: Firmware Trade Study Weighting

9.2.2 FirmWare Scale Assignment

Flight Control Firmware Criteria Standards					
Criteria	1	2	3	4	5
Functionality	Firmware cannot handle autonomous flight and is only for RC applications.	Control laws for both fixed-wing, transition modes, and hover mode have to be written from entirely from scratch.	Software and control laws require extensive modification. Firmware is difficult to physically interface with avionics package.	Requires some changes to software to interface with avionics package. Has standard control algorithms for configuration.	Capable of switching between horizontal and level flight modes out of box. Supports our specific configuration with advanced control algorithms.
Resources	No open-source information or tutorials. Hard to use software, does not interface with GSE software, language is complex.	Software/firmware cannot be altered GSE software does not work with the flight control system well. Some open source information	N/A.	Alterations to software is possible and fairly intuitive. Backed up with forums, tutorials, on website/online. Language is complex but understandable	Adjustable control through interface with GSE software. Language is simple and intuitive, resources for all flight modes can be found. Plentiful documentation
Customer Preference	Doesn't take into account the customers option used for ground station software. Would require significant alteration from customer's existing workflow	N/A	Interfaces with provided GSE Differs from existing platform used by customer but functionality is usable for mission.	Integrates into customers' choices for flight controller and ground control software.	Compatible with existing IRISS workflow, familiar to team for the purpose of further development
Hardware and Software	Functions on only specific operating systems, requiring the purchasing. Requires significant reworking of software.	N/A	Interfaces with provided GSE hardware with minimal extra hardware to purchase. Requires creating basic UI, some learning curve to software.	N/A	Doesn't require any additional hardware for operation besides what will be provided Fully developed UI, plug-n-play functionality, easily understandable software.

Table 10: Scale Assessment of Flight Controller Firmware Criteria

9.3 Battery Chemistry Design

9.3.1 Battery Chemistry Criteria and Weight Assignment

Criteria	Weight (%)	Rationale
Energy Density	25	High energy density is critical to have the highest battery capacity while maintaining the lowest weight, which allows the aircraft to achieve a one hour flight time with a lightweight aircraft.
Discharge Rate	20	The ability of the battery to provide enough current for the high demands of VTOL functionality - in order to produce enough power, the battery and wiring system must be capable of handling sufficient current.
Cost	20	Battery cost tends to correspond directly with performance, and a high performance battery will be more expensive. Although this performance is essential to the project, there is a limited project budget. The cost will be a large limiting factor, but performance is weighted higher than cost.
Lifespan	20	A cycle of a battery is defined as a full battery being discharged to empty and charged to full capacity again. Over time after charging and discharging the battery so many times, the capacity of the battery will slowly decrease. The lifespan of the battery is the number of cycles that the battery can go through before it needs to be replaced where maximizing the number of cycles is important so that a new battery does not need to be purchased as often.
Safety	15	Different battery types have different discharge properties. Some batteries may become unusable if they drop below a certain voltage. Other batteries may be dangerous to the user, so proper safety precautions must be made. Because of this, safety is weighted low because vehicle performance takes precedent.
Total	100	

Table 11: Trade Study Battery chemistry Weighting

9.3.2 Battery Chemisty Scale Assignmment

Battery Chemistry Criteria Standards					
Criteria	1	2	3	4	5
Discharge Rate (per cell)	0.5C	1C	2C	5C	10C
Energy Density	0-30 Wh/kg	30-60 Wh/kg	60-90 Wh/kg	90-120 Wh/kg	> 120 Wh/kg
Cost (per cell)	250 \$/kWh	200 \$/kWh	150 \$/kWh	100 \$/kWh	50 \$/kWh
Lifespan (discharge cycles)	Battery shows significant wear (loss of charge capacity) after 250 or fewer cycles	Battery lasts 250-500 discharge cycles without significant capacity loss	Battery lasts 500-750 discharge cycles without significant capacity loss	Battery lasts 750-1000 discharge cycles without significant capacity loss	Battery lasts 1000 or more cycles without showing significant degradation of charge capacity
Safety	Battery presents a high risk to the user - sensitive to overcharging, overheating, impacts, etc.	N/A	Battery is safe if handled and stored according to manufacturer's instructions, low risk of overcharging or damaging at low charge states	N/A	Battery is very safe - Can withstand extreme conditions, impacts, etc.

Table 12: Scale Assessment of Battery Composition

9.3.3 VTOL Criteria and Weight Assignment

Criteria	Weight (%)	Rationale
Risk	20	The risk associated with each configuration is a big factor in deciding which to use. Risk grows with the number of potential failures from added structures and components, or the general technical complexity of systems.
Manufacturing/Complexity	15	How many modifications and the time required to do them a is critical criteria.
Weight	10	Number of added structural components and motors greatly effect the total weight of the system, which is important to keep in mind when attempting to fly.
Hover Control	20	A configuration's control during VTOL mode is a deciding factor as steady level hover is a design requirement.
Cruise Efficiency	30	The configurations complexity, power draw, weight, and more will have direct impacts on cruise efficiency. A 1 hour cruise endurance is a critical project element.
Cost	5	The customer has provided a budget for per-unit cost on a finished product, but the budget may have some flexibility and is thus weighted lightly with respect to the other sections.
Total	100	

Table 13: Rotor Configuration Weighting

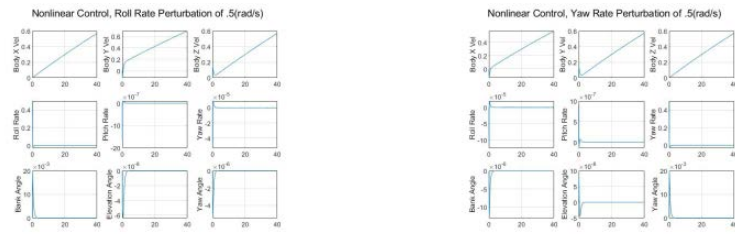
9.3.4 VTOL Scale Assignment

Due to the nature of many criteria being hard to assign objective values to at this point, the values were assigned to each option relative to the other options in the study. For the options reading "N/A", values were interpolated between the other options. Cost refers to the additional hardware that is required to allow VTOL configuration compared to a standard assembly of the Drak.

VTOL Configuration Criteria Standards					
Criteria	1	2	3	4	5
Risk	Many points of failure. VTOL system is technically complicated with many pieces.	N/A	Moderate amount of points of failure.	N/A	Minimal points of failure. Design is proven with extensive examples.
Manufacturing / Complexity	Requires difficult and time-consuming modification to aircraft body. Spars for tilting, spars/tails to hold rotors.	Requires modification to wings and bodies to hold rotors.	Moderate modifications, but requires a tail boom, or jutting structure.	N/A	Minimal modifications, ideally a bracket that can be simply put on. Makes use of existing mounting points in Drak wing kit.
Weight	Extensive additional structure	4 motors	3 motors, moderate additional structure	2 motors	1 motor, minimal additional structure
Hover Controllability	Minimal control authority from VTOL system. Easily destabilized, even in no wind.	N/A	Moderately control authority from VTOL system. Requires some modification of control software.	N/A	VTOL system has control authority with a wide margin in all conditions. Doesn't rely on control authority from control surfaces.
Cruise Efficiency	Many drag elements not contributing to propulsion.	N/A	Few drag elements not contributing to propulsion.	N/A	No drag elements not contributing to propulsion, few additional drag elements at all.
Cost	\$700 or more	\$500-\$700	\$300-\$500	\$100-\$300	\$100 or less

Table 14: Scale Assignment for VTOL Configuration

9.4 Hover Mode Controls



(a) Roll Perturbation Response

(b) Yaw Perturbation Response

Figure 47: Hover Mode Response to Other Perturbations

9.5 Level Flight Dynamics

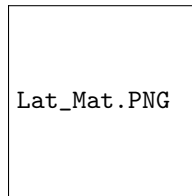


Figure 48: Linearized Lateral Matrix

Appendix B: Detailed Firmware Diagrams

Section Authors: Roland Ilyes

9.6 Diagrams

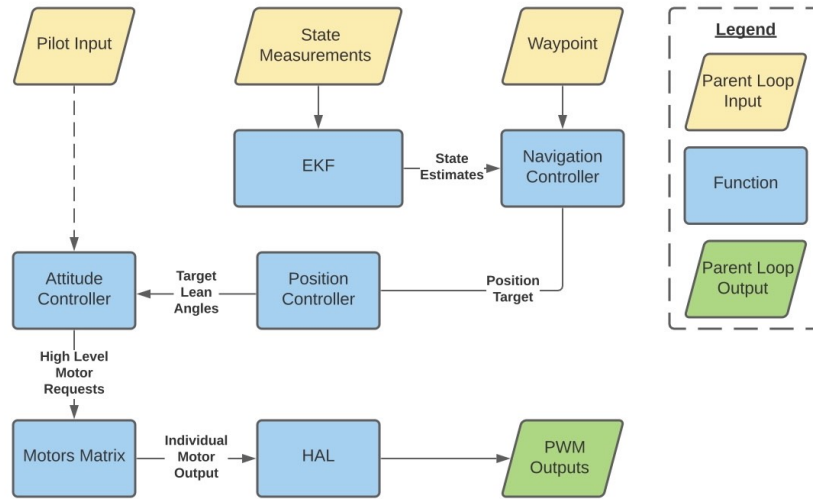


Figure 49: ArduCopter Parent Diagram

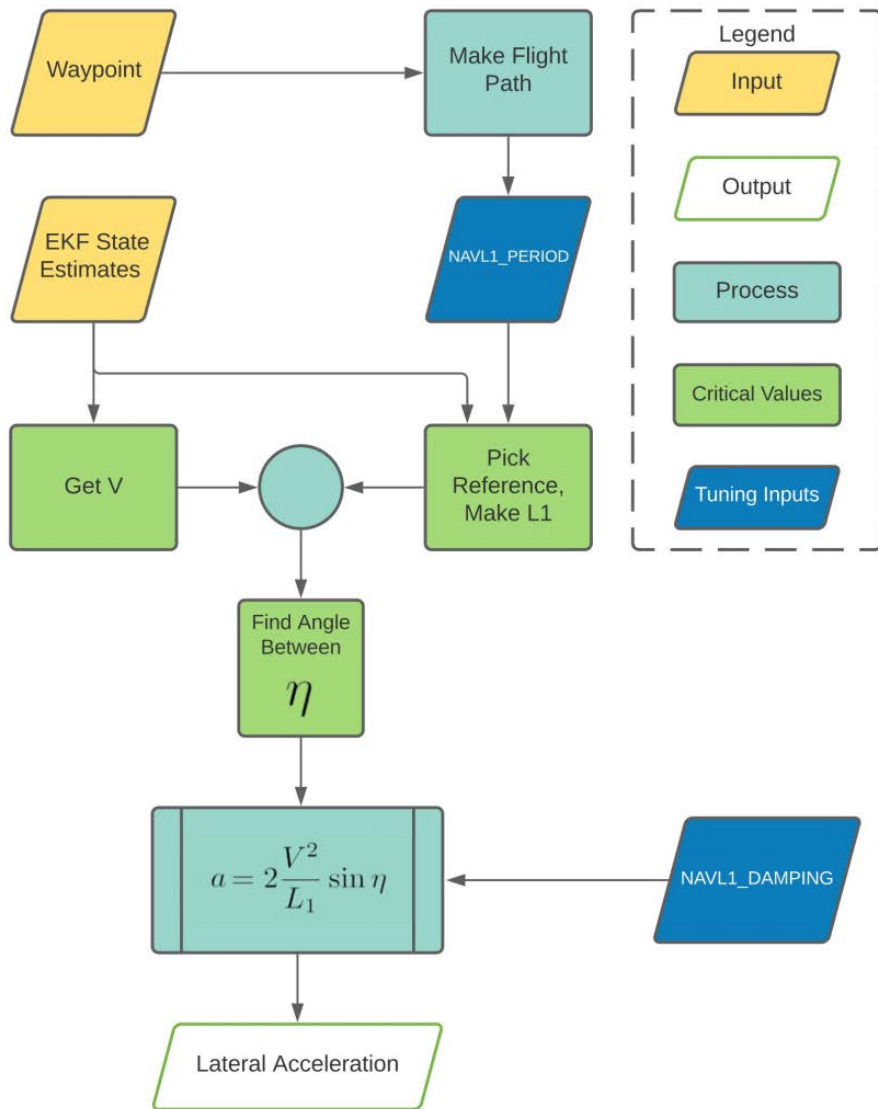


Figure 50: L1 Navigation Controller Functional Block Diagram

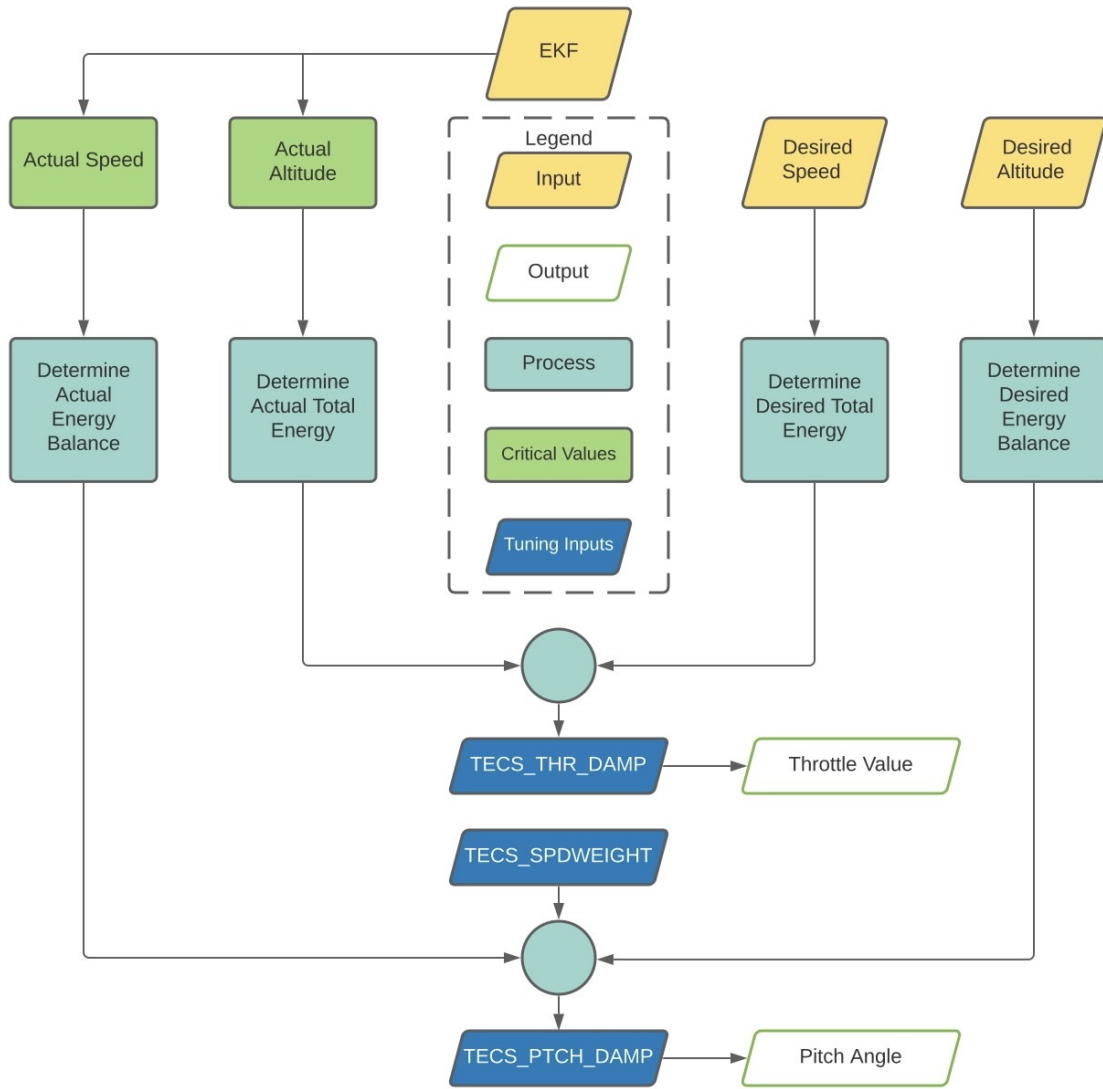


Figure 51: Total Energy Control System (TECS) Functional Block Diagram